Substrate potential of last interglacial to Holocene permafrost organic matter for future microbial greenhouse gas production

Janina G. Stapel[1], Georg Schwamborn[2], Lutz Schirrmeister[2], Brian Horsfield[1], Kai Mangelsdorf[1]

[1]GFZ, German Research Centre for Geoscience, Helmholtz Centre Potsdam, Organic Geochemistry, Telegrafenberg, 14473 Potsdam, Germany
[2]Alfred Wegener Institute, Helmholtz Centre for Polar and Marine Research, Department of Periglacial Research, Telegrafenberg, A43, 14473 Potsdam, Germany

Correspondence to: Janina G. Stapel (Janina.stapel@gfz-potsdam.de)

Abstract. Multiple permafrost cores from Bol´shoy Lyakhovsky Island in NE Siberia comprising deposits from the last interglacial to modern time are investigated to evaluate the potential of freeze-locked organic matter (OM) as a substrate for the production of microbial greenhouse gases from thawing permafrost deposits. Deposits from Late Pleistocene glacial periods (comprising MIS 3 and MIS 4) possess an increased aliphatic character and a higher amount of potential substrates, and therefore higher OM quality in terms of biodegradation compared to deposits from the last interglacial (assessed as Eemian, MIS 5e) as well as from the Holocene (MIS 1). To assess the potential of the individual permafrost deposits to provide substrates for microbially induced greenhouse gas generation, concentrations of free (present substrate pool) and bound (future substrate pool upon degradation) acetate as an appropriate substrate for methanogenesis are used. The highest free (in pore water and segregated ice) and bound (bound to the organic matrix) acetate-substrate pools of the permafrost deposits are observed within the interstadial MIS 3 and stadial MIS 4 period deposits. In contrast, deposits from the MIS 5e show only poor substrate pools. The MIS 1 deposits reveal a significant bound-acetate pool, representing a future substrate potential upon release during OM degradation. Biomarkers for past microbial communities (branched and isoprenoid GDGTs) show also highest abundance of past microbial communities during the MIS 3 and MIS 4 deposits, which indicates higher OM quality with respect to microbial degradation during time of deposition. On a broader perspective, Arctic warming will increase permafrost thaw and favour substrate availability from freeze-locked older permafrost deposits. Therefore, especially those deposits from MIS 3 and MIS 4 show a high potential for providing substrates relevant for microbial greenhouse gas production.

1 Introduction

The northern areas of the Eurasian landmass are underlain by permafrost, which is defined as ground that remains under 0 °C for at least 2 consecutive years (Washburn, 1980). These areas represent a large reservoir of organic carbon freeze-locked in the permafrost deposits (French, 2007; Zimov et al., 2009). Hugelius et al. (2014) estimated that about 1300 Pg (1 Pg = 10^{15} = 1 Gt) of soil organic carbon is stored in the upper 0-3 m in the northern circumpolar permafrost regions, which is highly

vulnerable to climate warming (Grosse et al., 2011; Schmidt et al., 2011; Mu et al., 2014). Today, Arctic summer temperatures are higher than in the past 400 years (Chapin III et al., 2005) and increases in ground temperature, changes in soil drainage, deepening of the active layer (seasonally thawed surface layer), spatial retreat of permafrost and changes in vegetation have already been reported for the Arctic as a consequence of northern hemisphere warming (Davidson and Janssens, 2006; Anisimov, 2007; Romanovsky et al., 2010; Mueller et al., 2015). During permafrost formation low temperatures, anoxic soil conditions and low rates of organic matter (OM) decomposition (Levy-Booth et al., 2007; Schimel and Schaeffer, 2012) resulted into high rates of OM accumulation (Kuhry et al., 2009; Zimov et al., 2009; Schirrmeister et al., 2011a). Thawing of permafrost promotes the accessibility of the formerly preserved OM and nutrients for microbial turnover again, which results in increased microbial activity and consequently in increased OM decomposition rates (Dutta et al., 2006; Schmidt et al., 2011). As observed in incubation experiments on permafrost samples of different ages (Waldrop et al., 2010; Lee et al., 2012; Lipson et al., 2012; Knoblauch et al., 2013; Schadel et al., 2014; Walz et al., 2017), degradation of this OM can lead to enhance microbial production and the release of greenhouse gases such as carbon dioxide and methane to the atmosphere (Wagner et al., 2003; Schuur et al., 2008; McGuire et al., 2009; Knoblauch et al., 2013) with its feedback on global warming and further permafrost degradation. Former studies on samples from Holocene deposits and on Late Pleistocene (LP) Yedoma deposits in, an ice-rich paleosol formation that is wide spread in NE Siberia, have shown that microbial degradability of the freeze-locked OM in permafrost seems to depend on the amount and quality of organic carbon rather than on the age of the deposits (Knoblauch et al., 2013; Strauss et al., 2015; Stapel et al., 2016).

NE Siberian permafrost formation started already in the Late Pliocene (e.g. at the todays coasts and islands along the Dmitry Laptev Strait (Arkhangelov et al., 1996)) and provides a unique paleo-environmental archive with stratigraphic patterns of long-lasting accumulation periods of permafrost during glacial periods, as well as permafrost degradation features during interglacial periods (Andreev et al., 2004, 2009; Wetterich et al., 2009, 2011). Here, permafrost deposits were accumulated under continental, cold climate conditions accompanied by syngenetic ice-wedge growth (Wetterich et al., 2011) during glacial periods, e.g. middle Pleistocene (Saalian) and Late Pleistocene (Weichselian; Yedoma deposits) (Andreev et al., 2004; Schirrmeister et al., 2013). In contrast, during the Eemian and the Holocene, extensive thawing of ice wedges and permafrost deposits led to the formation of thermokarst depressions, as well as of thermo erosional valleys and small rivers (Andreev et al., 2004; Ilyashuk et al., 2006; Wetterich et al., 2009). According to pollen and insect data, the climate of the Eemian resulted in an open grass and grass-sedge tundra similar to the modern one (Kienast et al., 2008), and the mid Eemian environment was characterized by summer temperatures up to 5 °C higher than modern with greater seasonal temperature variations in the Northern Hemisphere (Andreev et al., 2004; Dahl-Jensen et al., 2013).

As study area in NE Siberia Bol´shoy Lyakhovsky Island in the Laptev Sea was selected, since it provides the excellent opportunity to investigate permafrost OM deposited from last interglacial to Holocene time. The last interglacial deposits have been interpreted as Eemian deposits with, based on pollen data, 4-5 °C higher summer temperatures than today (Andreev et al., 2004). Especially, these Eemian deposits forming a paleo-equivalent to the Holocene interval are otherwise rather difficult to assess. According to prior studies by Wetterich et al. (2014) and references therein, the cores investigated

in this study can be integrated into an already described environmental and climatic history. It has to be mentioned that similar interglacial deposits at Oyogoss Yar from the mainland coast opposite to Bol'shoy Lyakhovsky Island have recently been dated and reveal younger latest infrared optical stimulated luminescence (IR-OSL) ages than Eemian (Opel et al., 2017). However, since it is not clear yet whether both deposits really represent the same age window, we stay here with the interpretation based on the Bol'shoy Lyakhovsky deposits by Andreev et al. (2004). To access information on quality in terms of biodegradability of the freeze-locked OM, we examined characteristic OM parameters (amount and quality) and low molecular weight organic acids (LMWOAs). LMWOAs such as acetate are important and easily convertible substrates for microbial metabolism (Ganzert et al., 2007) and are therefore used as a quality indicator in terms of future microbial degradability of the sedimentary OM (Glombitza et al., 2009; Strauss et al., 2015; Stapel et al., 2016). Acetate is a well-known substrate for methanogenesis (Chin and Conrad, 1995) and, thus its concentration provides information on the greenhouse gas production potential of the respective OM (Stapel et al., 2016). Acetate can either be dissolved in pore water and cryostructures (e.g. segregated ice) of permafrost deposits as free substrate being directly bioavailable for microorganisms or it can be bound to the organic matrix (e.g. by ester-linkage) forming a future substrate pool upon liberation via geochemical or microbial alteration of the OM (Glombitza et al., 2009; Stapel et al., 2016). In addition, investigations of microbial biomarkers such as phospholipid fatty acids (PLFAs) and glycerol dialkyl glycerol tetraethers (GDGTs) are used to examine present and past microbial communities in the context of modern and past environmental conditions. Phospholipids are essential membrane components of living cells (Zelles, 1999) and are hydrolysed rapidly after cell death (White et al., 1979; Logemann et al., 2011), therefore their fatty acid side chain inventories are used as an indicator for viable microorganisms in sediments (Haack et al., 1994). In contrast, GDGTs and archaeol represent membrane lipids of past microbial biomass, since they are already partly degraded as indicated by the loss of their head groups (Pease et al., 1998). While archaeol and GDGTs with isoprenoid tetraether bridges (iso-GDGTs) represent archaeal biomass, GDGTs with branched tetraether bridges (br-GDGTs) derive from bacteria (Weijers et al., 2006). However, in this context it should be mentioned that the br-GDGTs biomarkers only represent part of the bacterial community (Weijers et al., 2006; Schouten et al., 2013), while the archaeal markers cover most of the past archaeal community (Pancost et al., 2001; Koga and Morii, 2006).

The feedback between climate warming and microbial greenhouse gas generation from thawing permafrost is a topic of intensive modern scientific debate (Zimov et al., 2006; Koven et al., 2011; Schuur et al., 2015). Especially the contribution of OM from thawing permafrost deposits of different ages to the climate carbon feedback cycle is still an open question. Therefore, the aims of this study are (1) to compare the stored potential for microbial greenhouse gas production in permafrost deposits from different glacial/ interglacial and stadial/ interstadial periods, and (2) to assign the substrate potential of different permafrost units to characteristic OM parameters and palaeoenvironmental deposition conditions. Furthermore, the Eemian deposits in this study are used as model for an interglacial period containing information on how an ongoing warming climate in the Arctic may affect permafrost OM degradation.

2 Study area and material

Bol´shoy Lyakhovsky Island is located between the Laptev and East Siberian seas as the southernmost part of the New Siberian Archipelago (Fig. 1a). During Pleistocene periods of low sea level the island was part of west Beringia, an unglaciated landmass stretching from NE Siberia to Alaska (Hubberten et al., 2004; Andreev et al., 2009). The area is part of the northern tundra zone with an active layer thickness of 30-40 cm and a permafrost thickness of 500-600 m (Andreev et al., 2004). The study site is located west of the Zimov´e River mouth on the south coast of Bol´shoy Lyakhovsky Island along the Dmitry Laptev Strait (Fig. 1b). This southern coast is characterized by exposed permafrost deposits while the hinterland is formed by gradually sloping terrain intersected by rivers and valleys developed through thermo-erosion. Based on previous studies (Andreev et al., 2004, 2009; Ilyashuk et al., 2006; Kienast et al., 2008; Wetterich et al., 2009, 2014) in the study area the stratigraphy and regional setting are well known. Therefore, the drill sites (Fig. 1c) were chosen to maximize stratigraphic coverage and age with the aim to obtain a permafrost record from the Holocene (MIS 1) back to the Eemian interglacial (MIS 5e; Russian: Kazansevo).

The field work was conducted in April 2014 as part of the joint Russian-German research project CarboPerm (Schwamborn and Wetterich, 2015). Four cores were drilled using a KMB-3-15M (rotary) drill rig. The drilled core segments were kept frozen and transported in frozen state for further processing to Potsdam, Germany. In the home laboratory sampling was conducted in a climate chamber at -10 °C. 40 inner core samples distributed throughout the cores were taken with exception of intervals where ice-wedge ice was encountered. Samples were investigated for microbial biomarkers, free (pore-water) and bound acetate concentrations, and OM characteristics such as total organic carbon (TOC), total organic carbon to total nitrogen (TOC/TN) ratio, hydrogen index (HI) and compositional OM analysis using open-pyrolysis gas chromatography (Pyr-GC).

2.1 Core descriptions

Cores are described stratigraphically from younger to older deposits. Core L14-05 (Fig. 1c, Table 1) is 7.89 m long and consists of silty fine-grained sediments with scattered organic remains. Overall this core possesses lens-like cryostructures which are distinct between 1.00 to 2.45 m and 6.71 to 7.89 m core depth. According to prior studies by Andreev et al. (2009) and Wetterich et al. (2009), the upper core section approximately down to 5.5 m consists of a Holocene (MIS 1) unit, while the deeper deposits are of MIS 3 age (Russian: Kargin). According to previous paleo-environmental interpretations the MIS 1 deposits represent Alas deposits, where Early Holocene lake sediments have accumulated on top of a MIS 3 surface. During late Holocene time (<3.7 ka BP) the site drained and froze over.

Core L14-02 (Table 1) is 20.02 m in length. The upper 11.26 m consist of silty fine-grained sediments with macroscopical organic remains and an alternation of horizontal, vertical and reticulated ice veins, and lens-like cryostructures. Below 11.26 m the core consists of an ice wedge, and no samples were taken from this part. The core material is of Late Pleistocene age

and was deposited under subaerial conditions during the last interstadial MIS 3 (Wetterich et al., 2014). The deposits represent the infill of an ice-wedge polygon with a succession of paleosols.

The upper 4.90 m of core L14-03 (15.49 m in length; Table 1) are comparable in their sedimentology and cryostructures to the silty fine-grained sediments of core L14-02. Below 4.90 m the sediment has more sandy portions. The sediments between 4.90 to 8.45 m have visible organic remains and similar cryostructures. Below 8.45 m the sediments are characterized by only scattered organic remains but similar cryostructures as described above. Below 10.90 m the deposits mainly consist of sand and gravel, and in the lowermost 40 cm of gravel. Cryostructures are partly formed as vertically aligned cm-thick ice veins. In earlier studies at the same site these deposits are interpreted to represent MIS 4 (Russian: Zyryan) deposits (Andreev et al., 2009).

Core L14-04 (Table 1) is 8.10 m long and consists of silty fine-grained sediments with visible organic remains and cryostructures comparable to core L14-02. Between 4.24 to 4.89 m the core consists of massive ice. The upper 6 m were probably deposited during the MIS 4 stadial period. The deposits below 6 m were deposited during the Eemian (MIS 5e; Russian: Kazansevo) and appear to represent thermokarst lake sediments (Andreev et al., 2004).

3 Methods

3.1 Organic matter parameters

After freeze-drying and grinding the samples for total organic carbon (TOC) analysis were decalcified. TOC and total nitrogen (TN) (wt%) were determined by a carbon-nitrogen-sulphur analyser (Vario EL III, Elementar) with a device-specific accuracy of ± 0.1 wt%. For further information on characteristic OM parameters the hydrogen index (HI) was determined by Rock-Eval pyrolysis using a Rock-Eval 6 instrument (Behar et al., 2001). Therefore, 17 freeze-dried and ground samples of different TOC content covering all time intervals were analysed. Measurements were conducted by Applied Petroleum Technology AS (Kjeller, Norway). To obtain additional information on the macromolecular structure of the OM, 10 mg from the 17 selected samples were used for open-system pyrolysis after Horsfield et al. (1989). After the free biomolecules (bitumen) were thermally removed (300 °C), the macromolecular organic matrix was pyrolyzed with temperatures between 300-600 °C. The pyrolysates were trapped (liquid N_2) and finally measured on a pyrolysis-gas chromatograph (AGILENT GC 6890A Chromatograph) equipped with a flame ionization detector (Py-GC-FID). For peak quantification of the detected pyrolysate products *n*-butane was used as external standard. The areas of the detected pyrolysate peaks were integrated and calculated using the AGILENT ChemStation software. For the Eglinton-diagram (Eglinton et al,. 1990) o-xylene, 2,3-dimethylthiophene and *n*-nonene and for the Horsfield-diagram Horsfield et al. (1989) C_1-C_5 gases, C_6-C_{14}-*n*-alkanes and *n*-alkenes as well as C_{15} and longer *n*-alkanes and *n*-alkenes were integrated. For further details on the listed methods see Horsfield et al. (1989) and Stapel et al. (2016).

3.2 Low molecular weight organic acids (LMWOAs) analyses

After slow thawing of a subset of the frozen samples at about 4 °C, the pore water within the samples was separated by centrifugation (Sigma, laboratory centrifuge 6K15, 2500 rpm (908 x g), 20 °C, 10 min). Free LMWOAs such as acetate and anions were measured by ion chromatography with conductivity detection (ICS 3000, Dionex). Furthermore, LMWOAs bound via ester-bonds to the complex OM were analysed by conducting an alkaline ester cleavage approach developed by Glombitza et al. (2009a) on pre-extracted sediment samples. Details are described in Stapel et al. (2016).

3.3 Microbial lipid biomarker analysis

Approximately 30-50 g of the freeze-dried and ground samples were extracted using a flow blending system modified after Bligh and Dyer (1959) as described in Stapel et al. (2016). Subsequently, the obtained sediment extract was separated into four different fractions of increasing polarity (low polar lipids, free fatty acids, glycolipids, and polar lipids) following a method described by Zink and Mangelsdorf (2004). Finally, all four fractions were evaporated to dryness and stored at -20 °C until analysis. After a fatty acid cleavage procedure described in Müller et al. (1998), the phospholipid fatty acids (PLFA) within the polar-lipid fraction were measured by gas chromatography-mass spectrometry (GC-MS). For PLFA quantification an internal standard (1-myristoyl-d27-sn-glycero-3-phosphocholine) was used. Bacterial PLFAs from 14:0 to 21:0 with corresponding *iso*- and *anteiso*-FAs as well as br- and unsaturated-FAs have been measured. Details on instrument settings are described in Stapel et al. (2016).

After asphaltene precipitation the low polar-lipid fraction was separated into an aliphatic, aromatic and hetero-compound (containing nitrogen, oxygen and sulphur-components; NSO) fraction using a medium-pressure liquid chromatography system (MPLC) (Radke et al., 1980). An aliquot of the NSO fraction was investigated for tetraether lipids (glycerol dialkyl glycerol tetraether; GDGT) and archaeol using a Shimadzu LC20AD HPLC instrument coupled to a Finnigan TSQ 7000 triple quadrupole MS with an atmospheric pressure chemical ionization (APCI) interface. An external archaeol standard was used for quantification. Details on instrument settings are described in Stapel et al. (2016). The branched vs. isoprenoid tetraether (BIT) index were calculated after Hopmans et al. (2004). The data are provided in the supplement (table S1).

3.4 Statistical approaches

For testing optical correlations between the individual parameters, the Pearson correlation coefficient (R^2) was computed using the MATLAB R2015b software environment. In addition, p-values were also calculated with the same software and only correlations with $p \leq 0.05$ were evaluated for this study.

4 Results

Characteristic OM parameters (TOC and TOC/TN), biomarkers for living microbial communities (PLFA), past bacterial (br-GDGTs), past archaeal communities (iso-GDGTs-0 (no cyclopentyl-rings in the tetraether alkyl chains) and archaeol) as well

as the concentration of free and bound acetate are presented in figure 2 for all four cores from Bol´shoy Lyakhovsky Island. Every core includes at least one sample (core L14-03 has two samples) representing the overlaying soil as part of the active layer above the permafrost deposits from MIS 1, 3 and 4. Due to the stratigraphic settings at the study site on Bol´shoy Lyakhovsky Island, active layers containing OM from MIS 2 and MIS 5e could not be obtained in the field. Additionally, the results of 17 selected samples for open-system pyrolysis are shown in figure 3.

4.1 Characteristic OM parameters

Active layers:

In the active layers TOC values are slightly above 2.3 wt%, except in core L14-05 with 1.5 wt% (Fig. 2a). The TOC/TN values range between 8.2 and 11.1 (Fig. 2b). The representative active layer sample for Rock-Eval analysis revealed a hydrogen index (HI) of 236 mg HC/ g TOC (Fig. 2c). Overall, the samples reveal strongly increased PLFA concentrations (84.1, 149.3, 86.3 and 37.8 µg/g sediment, respectively) compared to the permafrost deposits below (Fig. 2d). The concentrations of br-GDGT (past bacterial markers) vary between 849.1, 53.2, 27.2 and 196.0 ng/g sediment, while the concentrations of the iso-GDGTs-0 + archaeol (past archaeal markers) are much lower with 20.7, 4.7, 5.3 and 6.1 ng/g sediment in each core, respectively (Fig. 2e,f). The free acetate concentration (Fig. 2g) is, compared to the rest of the cores, rather low (0.9 to 1.5 mg/l). In contrast, the bound acetate concentrations are comparatively high with 44.5 to 64.2 mg/l (Fig. 2h).

Marine Isotope Stage 1 (MIS 1):

In unit MIS 1 from core L14-05, the TOC, TOC/TN and HI-profiles (Fig. 2.a,b,c) correlate (TOC:TOC/TN, R^2=0.9; p=0.047 and TOC:HI, R^2=0.79; p=0.015). TOC values vary between 1.5 to 1.8 wt%, TOC/TN values between 7.1 to 8.2 and HI data between 71 to 194 mg HC/ g TOC (H1 to H5; Fig. 2c). Overall, the concentration of PLFAs is lower than in the active layer, ranging between 11 and 27 µg/g sediment (Fig. 2d). The PLFA profile revealed some similarities to TOC curve, but no overall correlation was found. Concentrations of past bacterial markers vary between 22.5 and 370.0 ng/g sediment, while past archaeal markers vary between 9.5 and 54.9 ng/g sediment (Fig. 2e,f). The br-GDGT profile correlates well with the TOC (R^2=0.9; p=0.015). Free acetate values (Fig. 2g) of about 2.2 mg/l were detected between 0.4 to 2.7 m, followed by an increase to 106 mg/l at 3.3 m depth. Bound acetate concentrations (Fig. 2h) correlate with TOC (R^2= 0.8; p=0.046) and are comparatively low (10.7 mg/l) at 0.4 m depth, but are much higher with values between 29.7 and 48.1 mg/l for the rest of the unit.

Marine Isotope Stage 3 (MIS 3):

Unit MIS 3 comprises the core segments MIS 3-1 of core L14-05, MIS 3-2 and MIS 3-3 of core L14-02 (Fig. 2). Overall, TOC and TOC/TN (Fig 2a,b) correlate (R^2=0.8; p=0.003). The core segment MIS 3-1 shows increased TOC (4.8 wt%) and TOC/TN (12.8) values, while core segment MIS 3-2 is characterized by TOC values of 1.4 to 4.7 wt% with a maximum at

1.6 m and TOC/TN values between 6.2 to 11.8. Within core segment MIS 3-3, TOC varies from 0.9 to 3.4 wt% and TOC/TN values range between 6.2 and 11.9. HI values of 316 (LP1), 322 (LP2) and 126 mg HC/ g TOC (LP3) are indicated for unit MIS 3 (Fig. 2c). Figure 2d shows PLFA concentrations of 33 µg/g sediment in core segment MIS 3-1, a decreasing trend from 11.1 to 35.6 µg/g sediment in core segment MIS 3-2, and values of 12.9 to 22.9 µg/g sediment in core segment MIS 3-3. In unit MIS 3 no correlation between PLFA concentrations and TOC is observable. The profile of past bacterial markers (Fig. 2e) in unit MIS 3 correlates with TOC (R^2=0.9; p=0.016). Past bacterial and archaeal biomarker (Fig. 2f) show higher abundances in the same depth interval, but the curves do not directly correlate (R^2= 0.8; p=0.021). In MIS 3-1 all past markers are strongly increased (2070.4 ng/g sediment for past bacterial GDGTs and 214.5 ng/g sediment for archaeal iso-GDGT-0 + archaeol). MIS 3-2 is characterized by concentrations of 34.4 to 591.1 ng/g sediment for the br-GDGTs and of 4.7 to 16.2 ng/g sediment for archaeal GDGT markers. Much lower concentrations of 3.5 to 147.7 ng/g sediment in the past bacterial profile, and concentrations of 1.3 to 31.7 ng/g sediment in the past archaeal profile are observed for MIS 3-3. Free acetate concentrations (Fig. 2g) of 51.1 mg/l are indicated for MIS 3-1, while in MIS 3-2 the free acetate concentrations rise to 412.0 mg/l at 1.6 m. In MIS 3-3 the highest free acetate concentrations of 757.5 mg/l are measured at 4.2 m, followed by decreasing values of 13.8 to 160.0 mg/l for the rest of the core segment. The bound acetate concentrations (Fig. 2h) correlate with TOC (R^2= 0.8; p=0.049) and show a concentration of 59.2 mg/l in MIS 3-1. Both, core segments MIS 3-2 and 3-3 reveal average concentrations of 11.7 to 49.1 mg/l with a maximum of 93.7 mg/l at 1.6 m and a maximum of 86.8 mg/l at 4.2 m.

Marine Isotope Stage 4 (MIS 4):

Unit MIS 4 is covered by core segments MIS 4-1 of core L14-03 and MIS 4-2 of core L14-04. TOC and TOC/TN values (Fig. 2a,b) correlate within unit MIS 4 (R^2=0.8; p=0.009). In core segment MIS 4-1 TOC values range between 2.7 to 1.9 wt% and the TOC/TN ratio between 8.6 and 9.7 in the upper 2.5 m, below TOC values are ≤ 1.5 wt% and TOC/TN values are < 6. Core segment MIS 4-2 is characterized by a decreasing TOC trend revealing values between 0.5 and 2.4 wt% and TOC/TN values between 4.5 and 9. Four HI values were measured in MIS 4-1 with values of 388 (LP4), 226 (LP5), 80 (LP6) and 256 mg HC/ g TOC (LP7) and one HI value of 276 mg HC/ g TOC (LP8) in MIS 4-2 (Fig. 2c). The PLFA concentrations (Fig. 2d) resemble TOC (R^2= 0.7; p=0.002) with values between 19.4 and 35.5 µg/g sediment in the upper 5 m of MIS 4-1 and lower concentrations of 5.2 to 10.0 µg/g sediment below 6 m. MIS 4-2 shows low PLFA concentrations of 8.1 to 19.2 µg/g sediment. In MIS 4-1 past microbial biomarker profiles (Fig. 2e,f) correlate with each other (R^2= 0.8; p=0.031) and with the TOC profile (br-GDGTs: TOC, R^2=0.7, p=0.047; iso-GDGTs-0 + archaeol: TOC, R^2=0.7, P=0.039). Here, the concentrations for bacterial markers range between 0.02 and 48.9 ng/g sediment with an increase from 149.1 to 208.0 ng/g sediment between 1.3 and 2.0 m, and at 4.7 m to 128.0 g/g sediment. For archaeal markers concentrations are between 0.6 and 6.6 ng/g sediment with a rise in concentration to 31.5 to 41.2 ng/g sediment between 1.3 and 2.0 m, and at 4.7 m to 11.9 ng/g sediment. In MIS 4-2 the bacterial GDGT concentrations are decreasing from 294.0 ng/g sediment to 34.2 ng/g sediment and correlate with TOC (R^2=0.9; p=0.018). The archaeal marker concentrations range between 7.8 and 18.5

ng/g sediment with a maximum at 5.3 and 6.3 m. The past archaeal GDGT marker and archaeol do not correlate with the profile of past bacterial GDGT markers or with TOC. Within core segment MIS 4-1 free acetate concentrations (Fig. 2g) were below 100.1 mg/l. However, extreme maxima occurred at 2.5 m (193.2 mg/l), and 6.4 m depth (628.5 mg/l). In core segment MIS 4-2 the free acetate concentrations range from 31.2 to 70.0 mg/l. The bound acetate concentrations (Fig. 2h) of unit MIS 4 resemble TOC (R^2=0.7; p=0.018) and usually are characterized by values of 6.7 to 23.7 mg/l with maxima between 2.0 to 3.4 m (40.5 to 61.8 mg/l) and at 5.7 m (44.6 mg/l) in MIS 4-1, and decreasing values from 41.7 to 12.1 mg/l in MIS 4-2.

Marine Isotope Stage 5e (MIS 5e):

In unit MIS 5e (Eemian) of core L14-04, TOC and TOC/TN correlate (R^2=0.99; p=0.018) and show values of about 0.6 wt% TOC and TOC/TN values from 3.7 to 4.9 (Fig. 2a,b). Samples from MIS 5e show HI values (Fig. 2c) of 61 (E1), 81 (E2) and 78 mg HC/ g TOC (E3). The PLFA concentrations (Fig. 2d) are between 4.5 to 5.2 µg/g sediment, which is quite low compared to the other intervals and resembles the TOC profile. Both past microbial marker profiles (Fig. 2e,f) correlate (R^2=0.9, p=0.036). The concentrations of past bacterial markers vary between 21.7 to 27.1 ng/g sediment, while the concentrations of the archaeal markers range from 3.4 to 5.2 ng/g sediment. The free acetate concentration (Fig. 2g) increases from 12.5 to 89.5 mg/l with depth, while the bound acetate concentration (Fig. 2h) scatters between of 0.5 to 19.6 mg/l.

4.2 Open system-pyrolysis GC

Results provided by open system-pyrolysis experiments on 17 representative samples (high/low TOC) enable a deeper insight into the OM characteristics:

Figure 3a (after Eglinton et al., 1990) classifies the deposited OM into aliphatic-, aromatic- or sulphur-rich OM. All samples from the Holocene (H1, H2, H3, H4, H5) and Eemian (E1, E2, E3) units and two samples from the Late Pleistocene unit (LP3, LP6) fall within the range of OM type III (terrestrial OM Type). Late Pleistocene samples (LP4, LP5, LP7, LP8) corresponding to higher HI values indicate a mixture of OM type III and II (increased aliphatic character). Two Late Pleistocene sample (LP1, LP2) and the active layer sample (AL), all displaying the highest HI values, fall within the range of OM type II indicating the strongest aliphatic character among all samples investigated. All samples, especially the samples from the Eemian (MIS 5e), show only a very low abundance of sulphur compounds generated by pyrolysis indicating sulphur lean OM (2,3-dimethylthiophene).

Figure 3b (after Horsfield et al., 1989) suggests different aliphatic characters for the selected samples, indicating an increasing aliphatic character with higher HI and TOC. Samples from the Eemian unit (E1, E2, E3) and the Holocene sample H1 as well as two samples from the Late Pleistocene unit (LP3, LP6) with low HI (< 130) and low TOC (< 1) reveal the weakest aliphatic character. In comparison, the samples from the Holocene unit (H2, H3, H4, H5) with intermediate HI (140-200) and TOC values > 1 show a slightly increased aliphatic character. All these samples are characterized by OM type III

(Fig. 3a). Most of the samples from the Late Pleistocene unit (LP1, LP2, PL4, PL5, PL6, PL7) and the active layer (AL) sample reveal the strongest aliphatic character corresponding to HI > 200 and to TOC >1 and to a mixture of OM type III and II (Fig. 3a).

5 Discussion

5.1 Organic matter characteristics

When permafrost thaws, formerly freeze-locked OM becomes bioavailable again (Wagner et al., 2007; Lee et al., 2012). In this context, it is of utmost interest for the assessment of the impact of this OM on future climate evolution not only to determine the abundance but also to learn more about the quality of the OM with regard to its potential degradability. For instance, terrestrial OM (more aromatic rich) is considered to be more recalcitrant than aquatic OM (more aliphatic rich) (Hedges et al., 2000). Although permafrost OM is mainly of terrestrial origin, also here the quality of the OM is determined by its different terrestrial sources and, therefore, structural composition as well as by its alteration due to early diagenetic degradation processes during its deposition in the past (White, 2013). In the following chapter we apply pyrolysis techniques (Rock-Eval pyrolysis and open-system pyrolysis GC-FID) on the OM to get a deeper insight into the structural composition and to establish a new tool for OM quality assessment as introduced in Stapel et al. (2016).

The permafrost deposits on Bol´shoy Lyakhovsky Island are dominated by terrestrial OM as indicated by the results of the open system-pyrolysis (Fig. 3a). This is supported by the BIT index-values ranging between 0.9 to 1 (table S1), which is based on the ratio of br-GDGTs and crenarchaeol and is close to one in soil OM (Hopmans et al., 2004). Samples from the active layer and the Late Pleistocene (LP) glacial period (comprising MIS 3 and MIS 4, Table 1) reveal in general a terrestrial OM source, however mixed with different proportions of aliphatic-rich OM. This is indicated by the results of the Rock-Eval (increased HI values; Fig 2c) and open-system pyrolysis (OM type II; Fig. 3a). The origin of this aliphatic-rich OM could be algae material, which is usually rich in aliphatic structural units (Kolattukudy, 1980). Thus, the samples with increased HI values might indicate OM accumulation during intervals of increased soil-moisture favourable for algae growth. Periods of increased soil moisture during the LP glacial period was already indicated by Sher et al. (2005). The highest accumulation of OM was found in the interstadial deposits of MIS 3 (core sections 3-1 and 3-2), with TOC values typical of Yedoma deposits (Schirrmeister et al., 2013). The measured TOC/TN values of 5 to 12 are within the range of terrestrial permafrost deposits reported for the NE Siberian Arctic (Wetterich et al., 2009; Schirrmeister et al., 2011a; Strauss et al., 2015). Usually, the TOC/TN ratio describes the amount of sedimentary OM that originates from aquatic vs. terrestrial sources and is commonly used to characterize the dominant origin of the OM (Meyers and Teranes, 2002). However, the TOC/TN signal can be overprinted by different processes during OM decomposition such as microbial consumption (preferred respiration of carbon vs. nitrogen) and pedogenic processes resulting in lower TOC/TN values for stronger decomposed OM (Carter and Gregorich, 2008). The HI is used as indicator for OM quality in terms of microbial degradability (Talbot and Livingstone, 1989; Stapel et al., 2016), since OM with a higher HI is considered to contain a

higher proportion of better degradable aliphatic molecular structures, whereas OM with a low HI contains a higher proportion of less degradable aromatic structures (Hedges et al., 2000). Thus, the low TOC and TOC/TN values (< 5), in addition to the low HI in the Eemian samples (MIS 5e, Table 1) may point to less favourable conditions for OM accumulation and/or an increased degree of OM decomposition and therefore to a reduced OM quality. This would be in line with the warmer and drier climate of the Eemian period in NE Siberia (Andreev et al., 2004; Wetterich et al., 2014; Wetterich et al., 2016), which might have supported intense aerobic microbial degradation of OM due to dyer soil conditions (Andreev et al., 2009). The last interglacial was characterized by higher summer temperatures compared to the LP glacial period (Bond et al., 2001; Shackleton et al., 2003; Kienast et al., 2008, 2011) and accompanied by permafrost thawing, draining, thermokarst formation and thermal erosion (Table 2) (Andreev et al., 2009).

The same conclusions can be drawn from the component-specific analysis of the OM by open system-pyrolysis GC (Fig. 3). Here, the Eemian deposits (E1, E2, E3) show a more pronounced terrestrial OM type III character due to their higher content of aromatic components and lower content of aliphatic components compared to the Holocene (MIS 1) deposits (except of sample H1; Fig. 3a). Furthermore, by examining their aliphatic compositions in more detail (Fig. 3b), the differences between the Eemian and Holocene interglacial deposits (both are interpreted to have comparable vegetation (Kienast et al., 2008)) are expressed by the higher aliphatic character and higher HI values of the Holocene deposits, which likely indicates less decomposed OM and higher OM quality in the Holocene compared to the Eemian deposits.

The LP glacial period (Yedoma deposits) was influenced by climate variations, which resulted into alternating wetter or drier environmental conditions in NE Siberia (Andreev et al., 2009). The generally cold climate and anaerobic soil conditions during the LP glacial period slowed rates of soil OM decomposition (Dutta et al., 2006) and increased the accumulation of OM (Andreev et al., 2011; Schirrmeister et al., 2011a; Wetterich et al., 2014). The Yedoma deposits (comprising MIS 3 and partly MIS 4) composed of terrestrial OM with a higher aliphatic proportion (Figs. 3a and 3b) are indicative for a depositional environment with increased soil-moisture during deposition. Here, a higher input of aliphatic-rich presumably aquatic OM (e.g. algae material) is accompanied by an increased accumulation of TOC and higher values of HI (LP1, LP2, LP4, LP5, LP7, LP8; Fig. 2). In contrast, those LP glacial period samples with lower TOC and HI values (LP3, LP6; Fig. 2) reveal a minor aliphatic character, which likely reflect a change to a drier depositional environment with less water-saturated soils at the respective time interval.

The effect of different depositional setting on the OM quality is not really clear yet. Our study suggests that OM deposited in soils from LP glacial time reveal a higher OM quality than the Holocene and Eemian OM deposited in thermokarst lake environments. However, since both Holocene and Eemian samples were deposited in comparable settings (thermokarst lakes), the significant difference in the OM parameters observed here indicate that environmental conditions might have a stronger impact on the OM characteristics than the depositional settings. Thus, more investigation on different depositional settings not only with depth and sediment age but also on a regional scale has to be conducted to improve our insights into the different factors determining the quality of OM in permafrost regions.

Overall, the results from the open system-pyrolysis suggest a terrestrial OM source for all investigated samples with varying proportions of aliphatic-rich OM affected by shifts in soil moisture as observed for the Yedoma deposits, and presumably higher rates of decomposed OM during dryer conditions as observed for the Eemian deposits. Furthermore, since HI values appear to resemble the varying aliphatic character of the OM in the permafrost deposits, HI seems to be an appropriate parameter to assess the quality of the OM supporting results presented in Stapel et al. (2016).

5.2 Signals of present and past microbial communities in permafrost deposits

In order to investigate whether the freeze-locked OM already stimulated a microbial community during deposition in the past, biomarkers for past microbial communities were examined. Since past microbial biomarkers could also be a product of microbial degradation of a presently living microbial community, the Bol´shoy Lyakhovsky samples were also screened with regard to microbial life markers to compare both biomarker records. As life markers we used phospholipids with ester bound fatty acids (PLFAs), since these bacterial cell membrane components are rapidly degraded after cell death (Logemann et al., 2011). In contrast, intact polar lipids (IPL) with ether bond moieties (e.g. archaeol) have only a restricted potential to act as life markers for archaea due to their significantly higher stability (Logemann et al., 2011). Thus, since microbial communities generally contain of bacteria and archaea we used the PLFAs here as a general indicator for intervals of increased microbial life.

PLFA life markers indicate the occurrence of a living bacterial community in the investigated deposits from Bol´shoy Lyakhovsky Island. While the PLFA signals are low in the permafrost deposits, all active layers contain higher amounts of PLFAs indicating a larger bacterial community in these surface layers. According to Knoblauch et al. (2013), permafrost surface layers contain both fresh and old OM (within the permafrost), which can stimulate microbial activity. The high concentrations of PLFAs in the active layers suggest that not only the abundance of microbial life is increased in these layers, but also the microbial activity. Living microbial cells in permafrost deposits are strongly decreased compared to the active layers and it has been hypothesized that these are most likely living successors of the microbial community incorporated into the sediments during time of deposition (Bischoff et al., 2013). Different studies have shown that these cells can be re-activated upon permafrost thaw, after which they are able to produce greenhouse gases (e.g. Knoblauch et al., 2013; Schuur et al., 2015; Treat et al., 2015; Walz et al., 2017).

Glycerol dialkyl glycerol tetraethers (GDGTs) and archaeol represent past microbial biomass (Stapel et al., 2016). GDGTs and archaeol are the cores of former membrane lipids, which are already partly degraded as indicated by the loss of their head group moieties. However, the core lipids are very stable over geological time scales (Pease et al., 1998; Schouten et al., 2013) and can be found in many different habitats (Bischoff et al., 2013; Schouten et al., 2013). Past bacterial (br-GDGTs (Weijers et al., 2006)) and archaeal (iso-GDGTs and archaeol (Koga et al., 1993; Pancost et al., 2001)) markers provide information on the abundance of a past microbial community and indirectly might say something about microbial activity during time of deposition. Iso-GDGT-0 (no cyclopentyl-rings in the tetraether alkyl chains) and archaeol are used as markers for methanogenic communities in permafrost regions (Pancost et al., 2011; Bischoff et al., 2014), although their relative

proportion vary within different methanogenic genera (Koga and Mori, 2006). PLFA life marker profiles only indicate abundant microbial life for the active layers and do not correlate with the past markers. Thus, the data suggest that in the permafrost sequence the past marker represent a paleo-signal (Stapel et al., 2016).

The results show that intervals with increased concentrations of past microbial markers often correspond to increased OM concentration (TOC) and quality (HI and higher aliphatic character). This can especially be observed in the Yedoma deposits of core sections MIS 3-1, 3-2 and in the upper part of 4-1 and 4-2 (Fig. 2c: LP1, LP2, LP4 and LP8). Thus, the data in this suggest (chapter 5.1) that the OM with higher quality seems to have stimulated an abundant microbial life during deposition in the past. Both bacterial and archaeal past markers are increased in these intervals (Figs 2e,f), whereas the archaeal markers suggest the presence of methanogenic communities and presumably greenhouse gas production in the past. Also if relating the past microbial markers to the TOC content of the sediments the same trends can be observed, indicating stimulated microbial communities at these depth intervals. Based on that, we suggest that the amount and quality of OM are responsible for the detected past bacterial and archaeal abundance in the Yedoma deposits (Fig. 2e,f).

In a future warmer climate, a slight increase in permafrost temperatures has not only an influence on the soil-moisture content but also on the abundance and diversity of the microbial community (Wagner et al., 2007). Thus, intervals of increased past-marker concentrations reveal time intervals of increased soil-moisture levels, which are thought to be linked to warmer surrounding temperatures (Stapel et al., 2016), especially during the MIS 3 and 4. This link was already observed by Bischoff et al. (2013). Here, comparable high concentrations of archaeol (up to approximately 40 ng/g sediment) and iso-GDGTs (up to approximately 20 ng/g sediment) were detected in Yedoma sediments, which were deposited during warmer and wetter environmental conditions in the Late Pleistocene. Similar average concentrations of iso-GDGT-0 + archaeol are also detected in this study for the MIS 3 and MIS 4 deposits. On the other hand, the relatively high concentrations of archaeol (up to approximately 80 ng/g sediment) in the Holocene sequence of the permafrost deposits from Kurungnakh Island (Bischoff et al., 2013) are not detected within the Holocene deposits of this study. This might be due a less aquatic influence on the Holocene deposits at Bol´shoy Lyakhovsky Island than on the permafrost deposits at Kurungnakh Island (Bischoff et al., 2013). Thus, these data reflect that increased soil moisture during deposition resulted in excellent living conditions for anaerobic bacteria (Weijers et al., 2006) and archaea (Wagner et al., 2007), especially during the MIS 3. According to Wetterich et al (2014), the MIS interstadial optimum occurred between 48 to 38 ka BP on Bol´shoy Lyakhovsky Island and is characterized by warmer temperature conditions with tundra environments with water-saturated active layers (Meyer et al., 2002; Hubberten et al., 2004; Andreev et al., 2011).

The Holocene (MIS 1) and Eemian (MIS 5e) deposits in this study were deposited in a different geomorphological environment than the Yedoma deposits referred to as thermokarst lakes (Andreev et al., 2004; 2009). According to Peterse et al. (2014), significantly higher concentrations of br-GDGTs (approximately 8800-47600 ng/g sediment) are found in flooded or water-filled permafrost depressions (e.g. thermokarst lake sediments) than in frozen Yedoma deposits (161 ng/g sediment). Nevertheless, the results of this study show similar high or even lower concentrations of br-GDGTs and iso-GDGTs (table S1) as well as archaeol in the deposits of MIS 1 and 5 compared to the LP glacial permafrost deposits, and an

average BIT index of 1 for all investigated deposits. Thus, although the geomorphological environment in the MIS 1 and 5 was described as thermokarst lakes (Andreev et a., 2004; 2009), the data indicate that these thermokarst lakes were probably only of minor durability and therefore did not affect significantly on the concentration of once living microorganisms (past marker).

5.3 Microbial substrate potential for greenhouse gas generation

Degradation of permafrost OM becoming bioavailable again in the course of ongoing permafrost thaw can finally lead to the production and release of greenhouse gases such as methane and carbon dioxide with their impact on the global climate cycle. To assess the potential of the OM from different depositional ages to provide substrates for the production of greenhouse gases, acetate is used as an appropriate substrate for microbial metabolism (Ivarson and Stevenson, 1964; Sørensen and Paul, 1971; Sansone and Martens, 1981; Balba and Nedwell, 1982). Acetate is the terminal electron acceptor for methanogens in cold-temperate environments (Chin and Conrad, 1995; Wagner and Pfeiffer, 1997), especially for acetoclastic methanogens (Thauer, 1998) and methanogenic archaea which are ubiquitous in anoxic environments and in permafrost sediments (Kobabe et al., 2004).

In this study two acetate pools are investigated: The free-acetate pool within the pore water, representing an easily accessible substrate source for microbial metabolism; and the bound-acetate fraction, which is still linked to the OM and constitutes a future substrate source upon degradation (Glombitza et al., 2009b). Overall, the concentrations of bound acetate (Fig. 2h) in the investigated samples correlate well with the amount of TOC and quality of OM. This indicates that larger reservoir pools for future microbial turnover exist at depths with increased TOC and HI (Fig. 2, Table 2). Deposits from the MIS 1, 3 and 4 possess increased bound acetate mean values, whereas the largest future substrate reservoir is located within MIS 3 (~ 48.9 mg/l), followed by MIS 4 (~ 33.26 mg/l) and MIS 1 (~30.05 mg/l) (Table 2). In contrast, the bound-acetate concentration in the Eemian (MIS 5e) deposits suggests a depleted and possibly already altered bound-substrate pool as the concentration is considerably lower (~ 9.98 mg/l) than in all other deposits.

The very low concentrations of free acetate and elevated concentrations of PLFA life markers detected in the investigated active layer samples suggest a higher microbial consumption of free acetate by an active microbial community (Lee et al., 2012; Knoblauch et al., 2013; Stapel et al., 2016). This activity is stimulated by e.g. warmer temperatures (thawing conditions) and the input of the fresh and old OM during the thawing period (Liebner et al., 2008). The thaw of permafrost due to global warming and the subsequent increase of active layer thickness result into the release of old organic carbon previously frozen in the permafrost, which is shown be particularly sensitive to temperature-induced microbial decomposition (Knorr et al., 2005; Davidson and Janssens, 2006), and therefore is considered as an important substrate source. In terms of the present study, the highest PLFA concentration was detected in the active layer above the MIS 3 deposits. This may reflect the high potential of the MIS 3 Yedoma deposits to serve as a substrate provider for a living microbial community upon thaw. In contrast, local environmental differences may also affect the PLFA concentration. For example, the core containing MIS 3 deposits was drilled on a stable tundra surface (core L14-02), while the other cores were

either drilled in a geomorphological dynamic terrace position experiencing thermo-erosion (Schirrmeister et al., 2011; Grosse et al., 2011) influenced by a seasonal input of sediment and water, or in a drained and refrozen Holocene thermokarst basin (core L14-05), which is characterized by lower ice contents and shallower active layers (Schwamborn and Wetterich, 2015). However, the increased PLFA concentrations in all active layers indicate to a certain extent that the permafrost deposits at least from MIS 3, 4 and 1 can serve as good substrate providers when thawed. For MIS 5e this could not be evaluated due to the lack of MIS 5e deposits with an active layer on top.

In contrast to the bound acetate concentrations, the free-acetate substrate pools and TOC content do not correlate well within each individual core (in all cores: $R^2 < 0.5$). The reason for this might be that free-acetate pool in permafrost pore waters is not only the result of acetate released from the OM, but also can be influenced by other factors e.g. lateral and vertical diffusion promoted by capillary pressure (Parlange, 1971), thawing and freezing processes as well as microbial production and consumption. However, positive relations between acetate (free and bound), TOC and HI are observed at several depth intervals mainly within the MIS 3 and 4 deposits (e.g. core L14-02 at 1.5 and 4.2 m, core L14-03 at 2.5 and 5.8 m). Here, the mean concentration (~ 93.6 and 82.1 mg/l) of free acetate is at least two to three times higher than that identified in the interglacial periods MIS 1 (24.1 mg/l) or MIS 5e (46.1 mg/l). The minor free-acetate pool in the Holocene deposits may be the result of the OM composition or of intense microbial consumption during OM deposition in the past as has been proposed for the modern active layer. The latter could be supported by deeper and prolonged thaw of active layers with increased active microbial acetate consumption (Xue et al., 2016) caused by the onset of the early Holocene, when warming resulted in unstable environmental conditions, especially during the Holocene Optimum (Andreev et al., 2004; Wagner et al., 2007; Wetterich et al., 2008). As such, the low concentrations of free acetate in the Eemian deposits may also be the result of increased microbial consumption due to warmer environmental conditions. Moreover, the Eemian is another period linked to permafrost thaw, which again likely altered the free-substrate concentrations in the sediment due to the lateral transport of water and/or sediment (Andreev et al., 2009). Based on the presented results obtained in this study it can be noted that sediments from the interglacial periods contain reduced amounts of free acetate in comparison to the LP glacial period investigated.

Changes in size of the free and bound acetate reservoirs are caused by either local microbial consumption or by lateral and vertical transport, probably also resulting in microbial acetate consumption on a larger scale (e.g. in a nearby located soil or lake). Although the free-acetate pool in the MIS 1 and MIS 5e deposits is similar low, the bound-acetate concentrations in the MIS 1 deposits imply that there exists a considerable future-substrate reservoir compared to the MIS 5e deposits (Table 2). On the other hand, in the investigated MIS 3 and 4 deposits both substrate pools (free and bound) are characterized by higher acetate concentrations compared to the deposits from the MIS 1 and 5 (Table 2). The deposits from the interstadial Yedoma period (MIS 3) in particular possess a larger substrate reservoir than found in other deposits linked to increased amount and quality of OM, as has been observed previously in a study of Buor Khaya Peninsula permafrost, 350 km SW from Bol'shoy Lyakhovsky Island (Stapel et al., 2016). Considering the sizeable thickness of the LP Yedoma deposit on Bol'shoy Lyakhovsky Island (20 m, Schennen et al., 2016) and across Siberia (10-60 m, Dutta et al., 2006), as well as its

extension across Russia (about 1028264 km^2, Grosse et al., 2013), it is hypothesised that a significant substrate pool may become accessible for future microbial greenhouse gas generation as permafrost thaws. On a broader perspective, ongoing warming in the Arctic will increase active layer thickness making substrates from deeper and older OM available for microbial decomposition, and enhancing the production and release of greenhouse gases (Schuur et al., 2008). Although the complexity of potential positive (e.g. Schuur et al. (2008)) and negative (e.g. Flanagan and Syed (2011)) feedback loops between climate warming and the carbon cycle in the Arctic is still uncertain, the permafrost substrate potential for future greenhouse gas production plays a key role concerning shifts in the microbial community composition, vegetation, hydrogeology and soil thermal regime. The results of this study suggest that OM deposited during the interstadial and glacial periods contain a larger substrate potential than that found in the interglacial deposits and that parameters deduced from OM pyrolysis seem to represent appropriate tools to reflect quality differences of the permafrost OM of different ages.

6 Conclusions

The quality of OM in terms of providing organic substrates for microbial induced greenhouse gas production varies within the investigated permafrost deposits from the Eemian to the present time and is controlled by environmental and climatic conditions. The strongest present and future substrate potential appears to be stored within the Yedoma OM deposits from the last interstadial (MIS 3) and stadial (MIS 4) period, which is characterized by increased HI values and a higher aliphatic character. Thus, this currently frozen Yedoma OM is likely to have a strong impact on the greenhouse gas driven climate-carbon feedback cycle when thawed. In contrast, the interglacial periods (Holocene and especially Eemian) show lower substrate potentials, which might point to stronger microbial degradation during deposition. The Eemian deposits reveal both low present and future substrate pools. However, the Holocene deposits at least contain a significant future-substrate pool, which may become available when recycled in the active layer.

Data availability

https://www.pangaea.de/ (follows after acceptance and includes all shown datasets)

Author contributions

J. G. Stapel performed the cores sub-sampling, the laboratory analyses and data interpretations guided by K. Mangelsdorf and B. Horsfield. G. Schwarmborn and L. Schirrmeister planned and coordinated the fieldwork, collected the cores and opened the cores. J. G. Stapel wrote the manuscript that all co-authors commented on.

Competing interests

The authors declare that they have no conflict of interest.

Acknowledgments

This research was supported by the German Ministry of Education and Research as part of the bilateral CarboPerm Project between Germany and Russia (grant no. 03G0836B). We thank all Russian and German participants of the drilling expedition, especially Mikhail N. Grigoriev (Melnikov Permafrost Institute, Yakutsk, Russia) for his leadership. We thank the three reviewers for their thoughtful and very constructive comments and suggestions on our manuscript.

References

Andreev, A. A., Grosse, G., Schirrmeister, L., Kuzmina, S. A., Novenko, E. Y., Bobrov, A. A., Tarasov, P. E., Ilyashuk, B. P., Kuznetsova, T. V., Brbetschek, M., Meyer, H. and Kunitsky, V.V.: Late Saalian and Eemian palaeoenvironmental history of the Bol´shoy;shoy Lyakhovsky Island (Laptev Sea region, Arctic Siberia), Boreas, 33(4), 319-348, doi: 10.1111/j.1502-3885.2004.tb01244.x, 2004.

Andreev, A. A., Grosse, G., Schirrmeister, L., Kuznetsova, T. V., Kuzmina, S. A , Bobrov, A. A., Tarasov, P. E., Novenko, E. Y., Meyer, H., Derevyagin, A. Y., Kienast, F., Bryantseva, A. and Kunitsky, V. V.: Weichselian and Holocene palaeoenvironmental history of the Bol´shoy Lyakhovsky Island, New Siberian Archipelago, Arctic Siberia, Boreas, 38(1), 72-110, doi: 10.1111/j.1502-3885.2008.00039.x, 2009.

Andreev, A. A., Schirrmeister, L., Tarasov, P. E., Ganopolski, A., Brovkin, V., Siegert, C., Wetterich, S. and Hubberten, H.-W.: Vegetation and climate history in the Laptev Sea region (Arctic Siberia) during Late Quaternary inferred from pollen records, Quaternary Science Reviews, 30(17), 2182-2199, doi: 10.1016/j.quascirev.2010.12.026, 2011.

Anisimov, O. A.: Potential feedback of thawing permafrost to the global climate system through methane emission, Environmental Research Letters, 2(4), 045016, doi:10.1088/1748-9326/2/4/045016, 2007.

Arkhangelov, A., Mikhalev, D. and Nikolaev, V.: Reconstruction of formation conditions of permafrost and climates in Northern Eurasia, History of Permafrost Regions and Periglacial Zones of Northern Eurasia and Conditions of Old Human Settlement"(AA Velichko, AA Arkhangelov, OK Borisova, et al., Eds.), 85-109, 1996.

Balba, M. T. and Nedwell, D. B.: Microbial metabolism of acetate, propionate and butyrate in anoxic sediment from Colne Point Saltmarsch, Essex, U.K., Journal of General Microbiology, 128(7), 1415-1422, doi: 10.1099/00221287-128-7-1415, 1982.

Beer, C.: Soil science: The Arctic carbon count, Nature Geoscience, 1(9), 569-570, doi: 10.1038/ngeo292, 2008.

Behar, F., Beaumont, V. and Penteado, H. D. B.: Rock-Eval 6 technology: performances and developments, Oil & Gas Science and Technology, 56(2), 111-134, doi:10.2516/ogst:2001013, 2001.

Bischoff, J., Mangelsdorf, K., Gattinger, A., Schloter, M., Kurchatova, A. N., Herzschuh, U. and Wagner, D.: Response of methanogenic archaea to Late Pleistocene and Holocene climate changes in the Siberian Arctic, Global Biogeochemical Cycles, 27(2), 305-317, doi: 10.1029/2011GB004238, 2013.

Bischoff, J., Mangelsdorf, K., Schwamborn, G. and Wagner, D.: Impact of Lake-Level and Climate Changes on Microbial Communities in a Terrestrial Permafrost Sequence of the El'gygytgyn Crater, Far East Russian Arctic, Permafrost and Periglacial Processes, 25(2), 107-116, doi: 10.1002/ppp.1807, 2014.

Bligh, E. G. and Dyer, W. J.: A rapid method of total lipid extraction and purification, Canadian journal of biochemistry and physiology, 37(8), 911-917, doi: 10.1139/o59-099, 1959.

Bond, G., Kromer, B., Beer, J., Muscheler, R., Evans, M. N., Showers, W., Hoffmann, S., Lotti-Bond, R., Hajdas, I. and Bonani, G.: Persistent solar influence on North Atlantic climate during the Holocene, Science, 294(5549), 2130-2136, doi: 10.1126/science.1065680, 2001.

Carter, M. R. and Gregorich, E. G.: Soil sampling and methods of analysis, Taylor and Francis, London, 1224 p, 2008.

Chapin III, F. S., Sturm, M., Serreze, C. M., McFadden, J. P., Key, J. R., Lloyd, A. H., McGuire, A. D., Rupp, T. S., Lynch, A. H., Schimel, J. P., Beringer, J., Chapman, W. L., Epstein, H. E., Euskirchen, E. S., Hinzman, L. D., Jia, G., Ping, C. L., Tape, K. D., Thompson, C. D. C., Walker, A. D. and Welker, J. M.: Role of Land-Surface Changes in Arctic Summer Warming, Science, 310(5748), 657-660, doi: 10.1126/science.1117368, 2005.

Chin, K.-J. and Conrad, R.: Intermediary metabolism in methanogenic paddy soil and the influence of temperature, FEMS microbiology ecology, 18(2), 85-102, doi: 10.1111/j.1574-6941.1995.tb00166.x, 1995.

Dahl-Jensen, D., Albert, M., Aldahan, A., Azuma, N., Balslev-Clausen, D., Baumgartner, M., Berggren, A.-M., Bigler, M., Binder, T. and Blunier, T.: Eemian interglacial reconstructed from a Greenland folded ice core, NATURE, 493(7433), 489-494, doi: 10.1038/nature11789, 2013.

Davidson, E. A. and Janssens, I. A.: Temperature sensitivity of soil carbon decomposition and feedbacks to climate change, NATURE, 440(7081), 165-73, doi: 10.1038/nature04514, 2006.

Dutta, K., Schuur, E. A. G., Neff, J. C. and Zimov, S. A.: Potential carbon release from permafrost soils of Northeastern Siberia, Global Change Biology, 12(12), 2336-2351, 2006.

Eglinton, T. I., Sinninghe Damsté, J. S., Kohnen, M. E. and de Leeuw, J. W.: Rapid estimation of the organic sulphur content of kerogens, coals and asphaltenes by pyrolysis-gas chromatography, Fuel, 69(11), 1394-1404, doi: 10.1016/0016-2361(90)90121-6, 1990.

Flanagan, L. B. and Syed, K. H.: Stimulation of both photosynthesis and respiration in response to warmer and drier conditions in a boreal peatland ecosystem, Global Change Biology, 17(7), 2271-2287, doi: 10.1111/j.1365-2486.2010.02378.x, 2011.

Fontaine, S., Barot, S., Barre, P., Bdioui, N., Mary, B. and Rumpel, C.: Stability of organic carbon in deep soil layers controlled by fresh carbon supply, NATURE, 450(7167), 277-280, doi: 10.1038/nature06275, 2007.

French, H. M.: The periglacial environment 3rd ed., John Wiley & Sons, Ltd, England, 2007.

Glombitza, C., Mangelsdorf, K. and Horsfield, B.: Maturation related changes in the distribution of ester bound fatty acids and alcohols in a coal series from the New Zealand Coal Band covering diagenetic to catagenetic coalification levels, Organic Geochemistry, 40(10), 1063-1073, doi: 10.1016/j.orggeochem.2009.07.008, 2009a.

Glombitza, C., Mangelsdorf, K. and Horsfield, B.: A novel procedure to detect low molecular weight compounds released by alkaline ester cleavage from low maturity coals to assess its feedstock potential for deep microbial life, Organic Geochemistry, 40(2), 175-183, doi: 10.1016/j.orggeochem.2008.11.003, 2009b.

Grosse, G., Schirrmeister, L., Siegert, C., Kunitsky, V. V., Slagoda, E. A., Andreev, A. A. and Dereviagyn, A. Y.: Geological and geomorphological evolution of a sedimentary periglacial landscape in Northeast Siberia during the Late Quaternary, Geomorphology, 86(1-2), 25-51, doi: 10.1016/j.geomorph.2006.08.005, 2007.

Grosse, G., Romanovsky, V., Jorgenson, T., Anthony, K. W., Brown, J., Overduin, P. P. and Wegener, A.: Vulnerability and feedbacks of permafrost to climate change, EOS, Transactions American Geophysical Union, 92, 73-74, doi: 10.1029/2011eo090001, 2011.

Grosse, G., Robinson, J. E., Bryant, R., Taylor, M. D., Harper, W., DeMasi, A., Kyker-Snowman, E., Veremeeva, A., Schirrmeister, L. and Harden, J.: Digital database of the distribution of late Pleistocene ice-rich syngenetic permafrost of the Yedoma Suite in East and Central Siberia, Russia, U.S. Geological Survey Open-File Report, 1-37 (1078), 2013.

Haack, S. K., Garchow, H., Odelson, D. A., Forney, L. J. and Klug, M J.: Accuracy, Reproducibility, and Interpretation of Fatty Acid Methyl Ester Profiles of Model Bacterial Communities, Applied and Environmental Microbiology, 60(7), 2483-2493, 1994.

Hedges, J. I., Eglinton, G., Hatcher, P. G., Kirchman, D. L., Arnosti, C., Derenne, S., Evershed, R. P., Kögel-Knabner, I., de Leeuw, J. W., Littke, R., Michaelis, W. and Rullkötter, J.: The molecularly-uncharacterized component of nonliving organic matter in natural environments, Organic Geochemistry, 31(10), 945-958, doi: 10.1016/S0146-6380(00)00096-6, 2000.

Horsfield, B., Disko, U. and Leistner, F.: The micro-scale simulation of maturation: outline of a new technique and its potential applications, Geologische Rundschau, 78(1), 361-373, doi: 10.1007/BF01988370, 1989.

Hubberten, H. W., Andreev, A. A., Astakhov, V. I., Demidov, I., Dowdeswell, J. A., Henriksen, M., Hjort, C., Houmark-Nielsen, M., Jakobsson, M., Kuzmina, S., Larsen, E., Lunkka, J. P., Lysa, A., Mangerud, J., Möller, P., Saarnistov, M., Schirrmeister, L., Sher, A. V., Siegert, C., Siegert, M. J. and Svendsen, J. I.: The periglacial climate and environment in northern Eurasia during the Last Glaciation, Quaternary Science Reviews, 23(11-13), 1333-1357, doi: 10.1016/j.quascirev.2003.12.012, 2004.

Hugelius, G., Strauss, J. Zubrzycki, S., Harden, J. W., Schuur, E. A. G., Ping, C. L., Schirrmeister, L., Grosse, G., Michaelson, G. J., Koven, C. D., O´Donnell, J. A., Elberling, B., Mishra, U., Camill, P., Yu, Z., Palmtag, J. and Kuhry, P.: Estimated stocks of circumpolar permafrost carbon with quantified uncertainty ranges and identified data gaps, Biogeosciences, 11(23), 6573-6593, doi: 10.5194/bg-11-6573-2014, 2014.

Ilyashuk, B. P., Andreev, A. A., Bobrov, A. A., Tumskoy, V. E. and Ilyashuk, E. A.: Interglacial History of a Palaeo-lake and Regional Environment: A Multi-proxy Study of a Permafrost Deposit from Bol'shoy Lyakhovsky Island, Arctic Siberia, Journal of Paleolimnology, 35(4), 855-872, doi: 10.1007/s10933-005-5859-6, 2006.

Ivanov, O.: Stratigrafiya i korrelatsiya Neogenykh i Chetvertichnykh otlozheniyakh subarkticheskikh ravnin Vostochnoi Yakutii (Stratigraphy and correlation of Neogene and Quaternary deposits of subarctic plains in Eastern Yakutia), Problemy izucheniya Chetvertichnogo perioda (Problems of the Quaternary Studies). InNauka, Moscow, 202-211, 1972.

Ivarson, K. and Stevenson, I.: The decomposition of radioactive acetate in soils: II. The distribution of radioactivity in soil organic fractions, Canadian journal of microbiology, 10(5), 677-682, doi: 10.1139/m64-087, 1964.

Kienast, F., Tarasov, P., Schirrmeister, L., Grosse, G. and Andreev, A. A.: Continental climate in the East Siberian Arctic during the last interglacial: Implications from palaeobotanical records, Global and Planetary Change, 60(3-4), 535-562, doi: 10.1016/j.gloplacha.2007.07.004, 2008.

Kienast, F., Wetterich, S., Kuzmina, S., Schirrmeister, L., Andrev, A., Tarasov, P., Nazarova, L., Kossler, A., Frolova, A., Kunitsky, V. V.: Paleontological records indicate the occurrence of open woodlands in a dry inland climate at the present-day Arctic coast in western Beringia during the last interglacial, Quaternary Science Reviews, 30, 2134-2159, doi:10.1016/j.quascirev.2010.11.024, 2011.

Knoblauch, C., Beer, C., Sosnin, A., Wagner, D. and Pfeiffer, E.-M.: Predicting long-term carbon mineralization and trace gas production from thawing permafrost of Northeast Siberia, Glob Chang Biol, 19(4), 1160-1172, doi: 10.1111/gcb.12116, 2013.

Knorr, W., Prentice, I. C., House, J. I. and Holland, E A.: Long-term sensitivity of soil carbon turnover to warming, NATURE, 433(7023), 298-301, doi: 10.1038/nature03226, 2005.

Kobabe, S., Wagner, D. and Pfeiffer, E.-M.: Characterisation of microbial community composition of a Siberian tundra soil by fluorescence in situ hybridisation, FEMS microbiology ecology, 50(1), 13-23, doi: 10.1016/j.femsec.2004.05.003, 2004.

Koga, Y., Nishihara, M., Morii, H. and Akagawa-Matshushita, M.: Ether Polar Lipids of Methanogenic Bacteria: Structures, Comparative Aspects, and Biosyntheses, Microbiological Reviews, 57(1), 164-182, 1993.

Koga, Y. and Morii, H.: Special methods for the analysis of ether lipid structure and metabolism in archaea, Analytical biochemistry, 348(1), 1-14, 20096.

Kolattukudy, P. E.: Biopolyester membranes of plants: cutin and suberin, Science, 208(4447), 990-1000, 1980.

Koven, C. D., Ringeval, B., Friedlingstein, P., Ciais, P., Cadule, P., Khvorostyanov, D. V., Krinner, G. and Tarnocai, C.: Permafrost carbon-climate feedbacks accelerate global warming, Proceedings of the National Academy of Sciences, 108(36), 14769-14774, doi: 10.1073/pnas.1103910108, 2011.

Kuhry, P., Ping, C. L., Schuur, E. A., Tarnocai, C. and Zimov, S.: Report from the International Permafrost Association: carbon pools in permafrost regions, Permafrost and Periglacial Processes, 20(2), 229-234, doi: 10.1002/ppp.648, 2009.

Lawrence, D. M. and Slater, A. G.: A projection of severe near-surface permafrost degradation during the 21st century, Geophysical Research Letters, 32(4), doi: 10.1029/2005GL025080, 2005.

Lee, H., Schuur, E. A. G., Inglett, K. S., Lavoie, M. and Chanton, J. P.: The rate of permafrost carbon release under aerobic and anaerobic conditions and its potential effects on climate, Global Change Biology, 18(2), 515-527: doi: 10.1111/j.1365-2486.2011.02519.x, 2012.

Liebner, S., Harder, J. and Wagner, D.: Bacterial diversity and community structure in polygonal tundra soils from Samoylov Island, Lena Delta, Siberia, International Microbiology, 11, 195-202, doi: 10.2436/20.1501.01.60, 2008.

Liljedahl, A. K., Boike, J., Daanen, R. P., Fedorov, A. N., Frost, G. V., Grosse, G., Hinzman, L. D., Iijma, Y., Jorgenson, J. C., Matveyeva, N., Necsoiu, M., Raynolds, M. K., Romanovsky, V. E., Schulla, J., Tape, K. D., Walker, D. A., Wilson, C. J., Yabuki, H. and Zona, D.: Pan-Arctic ice-wedge degradation in warming permafrost and its influence on tundra hydrology, Nature Geoscience, 9, p. 312-318, doi:10.1038/ngeo2674, 2016.

Lipson, D. A., Zona, D., Raab, T. K., Bozzolo, F., Mauritz, M. and Oechel, W. C.: Water-table height and microtopography control biogeochemical cycling in an Arctic coastal tundra ecosystem, Biogeosciences, 9, 577-591, doi: 10.5194/bgd-8-6345-2011, 2012.

Logemann, J., Graue, J., Köster, J., Engelen, B., Rullkötter, J. and Cypionka, H.: A laboratory experiment of intact polar lipid degradation in sandy sediments: Biogeosciences, v. 8(9), p. 2547-2560, doi:10.5194/bg-8-2547-2011, 2011.

McGuire, A. D., Anderson, L. G., Christensen, T. R., Dallimore, S., Guo, L., Hayes, D. J., Heimann, M., Lorenson, T. D., Macdonald, R. W. and Roulet, N.: Sensitivity of the carbon cycle in the Arctic to climate change, Ecological Monographs, 97(4), 523-555, doi: 10.1890/08-2025.1, 2009.

Meyer, H., Dereviagin, A., Siegert, C., Schirrmeister, L. and Hubberten, H.-W.: Palaeoclimate reconstruction on Big Lyakhovsky Island, north Siberia - hydrogen and oxygen isotopes in ice wedges, Permafrost and Periglacial Processes, 13(2), 91-105, doi: 10.1002/ppp.416, 2002.

Meyers, P. A. and Teranes, J. L.: Sediment organic matter, Tracking environmental change using lake sediments, Springer, p. 239-269, 2002.

Mu, C., Zhang, T., Schuster, P. F., Schaefer, K., Wickland, K. P., Repert, A. D., Liu, L., Schaefer, T. and Cheng, G.: Carbon and geochemical properties of cryosols on the North Slope of Alaska, Cold Regions Science and Technology, 100, 59-67, doi: 10.1016/j.coldregions.2014.01.001, 2014.

Mueller, C. W., Rethemeyer, J., Kao-Kniffin, J., Loppmann, S., Hinkel, K. M. and Bockheim, G.: Large amounts of labile organic carbon in permafrost soils of northern Alaska, Glob Chang Biol., 21(7), 2804-2817, doi: 10.1111/gcb.12876, 2015.

Müller, K. D., Schmid, E. N. and Kroppenstedt, R. M.: Improved identification of mycobateria by using the microbial identification system in combination with additional trimethylsulfonium hydroxide pyrolysis, Journal of Clinical Microbiology, 36(9), 2477-2480, 1998.

Opel T. Wetterich S., Meyer H., Dereviagin A. Yu., Fuchs M. C. and Schirrmeister L.: Ground-ice stable isotopes and cryostratigraphy reflect late Quaternary palaeoclimate in the Northeast Siberian Arctic (Oyogos Yar coast, Dmitry Laptev Strait), Clim. Past, 13, 587–611, doi.org/10.5194/cp-13-587-2017, 2017.

Pancost, R. D., Hopmans, E. C. and Sinninghe Damste, J. S.: Archaeal lipids in Mediterranean cold seeps: molecular proxies for anaerobic methane oxidation, Geochimica et Cosmochimica Acta, 65(10), 1611-1627, doi: 10.1016/S0016-7037(00)00562-7, 2001.

Pancost, R. D., McClymont, E. L., Bingham, E. M., Roberts, Z., Charman, D. J., Hornibrook, E. R. C., Blundell, A., Chambers, F. M., Lim, K. L. H. and Evershed, R. P.: Archaeol as a methanogen biomarker in ombrotrophic bogs, Organic Geochemistry, 42(10), 1279-1287; doi: 10.1016/j.orggeochem.2011.07.003, 2011.

Parlange, J.-Y.: Theory of water-movement in soils: I. one-demensional absorption, Soil science, v. 111(2), 134-137, 1971.

Pease, T. K., Van Vleet, E. S., Barre, J. S. and Dickins, H. D.: Simulated degradation of glyceryl ethers by hydrous and flash pyrolysis, Organic Geochemistry, 29(4), 979-988, doi: 10.1016/S0146-6380(98)00047-3, 1998.

Peterse, F., Vonk, J. E., Holmes, R. M., Giosan, L., Zimov, N. and Eglinton, T. I.: Branched glycerol dialkyl glycerol tetraethers in Arctic lake sediments: Source and implications for paleothermometry at high latitudes, JGR Biogeosciences, 119, 1738-1754, doi:10.1002/2014JG002639, 2014.

Radke, M., Willsch, H. and Welte, D. H.: Preparative hydrocarbon group type determination by automated medium pressure liquid chromatography, Anal. Chem., 52(3), 406-411, doi:10.1021/ac50053a009, 1980.

Romanovsky, V. E., Drozdov, D. S., Oberman, N. G., Malkova, G. V., Kholodov, A. L., Marchenko, S. S., Moskalenko, N. G., Sergeev, D. O., Ukraintseva, N. G., Abramov, A. A., Gilichinsky, D. A. and Vasiliev, A. A.: Thermal state of permafrost in Russia, Permafrost and Periglacial Processes, 21(2), 136-155, doi:10.1002/ppp.683, 2010.

Sansone, F. J. and Martens, C. S.: Methane production from acetate and associated methane fluxes from anoxic coastal sediments, Science, 211(4483), 707-709, doi:10.1126/science.211.4483.707, 1981.

Schadel, C., Schuur, E. A. G., Bracho, R., Elberling, B., Knoblauch, C., Lee, H., Luo, Y., Shaver, G. R. and Turetsky, M. R.: Circumpolar assessment of permafrost C quality and its vulnerability over time using long-term incubation data, Glob Chang Biol, 20(2), 641-52, doi: 10.1111/gcb.12417, 2014.

Schennen, S., Tronicke, J., Wetterich, S., Allroggen, N., Schwamborn, G. and Schirrmeister, L.: 3D ground-penetrating radar imaging of ice complex deposits in northern East Siberia, Geophysics, 81(1), WA195-WA202, doi: 10.1190/geo2015-0129.1, 2016

Schimel, J. and Schaeffer, S.: Microbial control over carbon cycling in soil. Front. Microbiol., 3(348), 155- 165, doi: 10.3389/fmicb.2012.00348., 2012.

Schirrmeister, L., Siegert, C., Kuznetsova, T. V., Kuzmina, S. A., Andreev, A. A., Kienast, F., Meyer, H. and Bobrov, A. A.: Paleoenvironmental and paleoclimatic records from permafrost deposits in the Arctic region of Northern Siberia, Quaternary International, 89(1), 97-118, doi: 10.1016/S1040-6182(01)00083-0, 2002.

Schirrmeister, L., Grosse, G., Wetterich, S., Overduin, P. P., Strauss, J., Schuur, E. A. G. and Hubberten, H.-W.: Fossil organic matter characteristics in permafrost deposits of the northeast Siberian Arctic, Journal of Geophysical Research, 116, doi: 10.1029/2011JG001647, 2011a.

Schirrmeister, L., Kunitsky, V., Grosse, G., Wetterich, S., Meyer, H., Schwamborn, G., Babiy, O., Derevyagin, A. and Siegert, C.: Sedimentary characteristics and origin of the Late Pleistocene Ice Complex on north-east Siberian Arctic coastal lowlands and islands – A review, Quaternary International, 241(1-2), 3-25, doi: 10.1016/j.quaint.2010.04.00, 2011b.

Schirrmeister, L., Froese, D., Tumskoy, V., Grosse, G. and Wetterich, S.: Yedoma: Late Pleistocene Ice-Rich Syngenetic Permafrost of Beringia, In: Elias S.A. (ed.) the Encyclopedia of Quaternary Science, 3, 542-552, doi: 10.1016/B978-0-444-53643-3.00106-0, 2013.

Schmidt, M. W., Torn, M. S., Abiven, S., Dittmar, T., Guggenberger, G., Janssens, I. A., Kleber, M., Kogel-Knabner, I., Lehmann, J., Manning, D. A., Nannipieri, P., Rasse, D. P., Weiner, S. and Trumbore, S. E.: Persistence of soil organic matter as an ecosystem property, NATURE, 478(7367), 49-56, doi: 10.1038/nature10386, 2011.

Schouten, S., Hopmans, E. C. and Sinninghe Damsté, J. S.: The organic geochemistry of glycerol dialkyl glycerol tetraether lipids: A review, Organic Geochemistry, 54, 19-61, doi:10.1016/j.orggeochem.2012.09.006, 2013.

Schuur, E. A., Bockheim, J., Canadell, J. G., Euskirchen, E., Field, C. B., Goryachkin, S. V., Hagemann, S., Kuhry, P., Lafleur, P. M., Lee, H., Mazhitova, G., Nelson, F. G., Rinke, A., Romanovsky, V. E., Shiklomanov, N., Tarnocai, C., Venevsky, S., Vogel, J. G. and Zimov, S. A.: Vulnerability of Permafrost Carbon to climate Change: Implications for the Global Carbon Cycle, Biogeosciences, 58, 701-714, doi: 10.1641/B580807, 2008.

Schuur, E. A., McGuire, A. D., Schädel, C., Grosse, G., Harden, W. J., Hayes, D. J., Hugelius, G., Koven, C. D., Kuhry, P., Lawrence, D. M., Natali, S. M., Olefeldt, D., Romanovsky, V. E., Schaefer, K., Turetsky, M. R., Treat, C. C. and Vonk, J. E.: Climate change and the permafrost carbon feedback, NATURE, 520(7546), 171-179, doi: 10.1038/nature14338, 2015.

Schwamborn, G. and Wetterich, S.: Russian-German Cooperation CARBOPERM: Field campaigns to Bol´shoy Lyakhovsky Island in 2014, Berichte zur Polar-und Meeresforschung, Alfred Wegener Insitute for Polar and Marine Research, Germany, 2015.

Shackleton, N. J., Sánchez-Goñi, M. F., Pailler, D. and Lancelot, Y.: Marine Isotope Substage 5e and the Eemian Interglacial, Global and Planetary Change, 36(3), 151-155, doi: 10.1016/S0921-8181(02)00181-9, 2003.

Sher, A. V., Kuzmina, S. A., Kuznetsova, T. V. and Sulerzhitsky, L. D.: New insights into the Weichselian environment and climate of the East Siberian Arctic, derived from fossil insects, plants, and mammals, Quaternary Science Reviews, 24(5), 533-569, doi: 10.1016/j.quascirev.2004.09.007, 2005.

Sørensen, L. H. and Paul, E.: Transformation of acetate carbon into carbohydrate and amino acid metabolites during decomposition in soil, Soil Biology and Biochemistry, 3(3), 173-180, doi:10.1016/0038-0717(71)90012-5, 1971.

Stapel, J. G., Schirrmeister, L., Overduin, P. P., Wetterich, S., Strauss, J., Horsfield, B. and Mangelsdorf, K.: Microbial lipid signatures and substrate potential of organic matter in permafrost deposits: Implications for future greenhouse gas production, Journal of Geophysical Research: Biogeosciences, 121(10), 2652-2666, doi: 10.1002/2016JG003483, 2016.

Strauss, J., Schirrmeister, L., Mangelsdorf, K., Eichhorn, L., Wetterich, S. and Herzschuh, U.: Organic-matter quality of deep permafrost carbon – a study from Arctic Siberia, Biogeosciences, 12(7), 2227-2245, doi:10.5194/bg-12-2227-2015, 2015.

Talbot, M. R., and Livingstone, D. A.: Hydrogen index and carbon isotopes of lacustrine organic matter as lake level indicators, Palaeogeography, Palaeoclimatology, Palaeoecology, 70, 121-137, doi:10.1016/0031-0182(89)90084-9, 1989.

Thauer, R. K.: Biochemistry of methanogenesis: atribute to Marjory Stephenson, Microbiology, 144(9), 2377-2406, 1998.

Treat, C. C., Natali, S. M., Ernakovich, J., Iversen, C. M., Lupascu, M., McGuire, A. D., Norby, R. J., Roy Chowdhury, T., Richter, A., Santruckova, H., Schadel, C., Schuur, E. A., Sloan, V. L., Turetsky, M. R. and Waldrop, M. P.: A pan-Arctic synthesis of CH4 and CO2 production from anoxic soil incubations, Global Change Biology, 21(7), 2787-2803, doi: 10.1111/gcb.12875, 2015.

Vonk, J. E., Tank, S. E., Bowden, W. B., Laurion, I., Vincent, W. F., Alekseychik, P., Amyot, M., Billet, M., Canario, J. and Cory, R. M.: Reviews and syntheses: Effects of permafrost thaw on Arctic aquatic ecosystems, Biogeosciences, 12(23), 7129-7167, doi: 10.5194/bg-12-7129-2015, 2015.

Wagner, D. and Pfeiffer, E.-M.: Two temperature optima of methane production in a typical soil of the Elbe river marshland, FEMS microbiology ecology, 22(2), 145-153, doi: 10.1111/j.1574-6941.1997.tb00366.x, 1997.

Wagner, D., Wille, C., Kobabe, S. and Pfeiffer, E.-M.: Simulation of freezing-thawing cycles in a permafrost microcosm for assessing microbial methane production under extreme conditions, Permafrost and Periglacial Processes, 14(4), 367-374, doi: 10.1002/ppp.468, 2003.

Wagner, D., Gattinger, A., Embacher, A., Pfeiffer, E.-M., Schloter, M. and Lipski, A.: Methanogenic activity and biomass in Holocene permafrost deposits of the Lena Delta, Siberian Arctic and its implication for the global methane budget, Global Change Biology, 13(5), 1089-1099, doi: 10.1111/j.1365-2486.2007.01331.x, 2007.

Waldrop, M. P., Wickland, K. P., White III, R., Berhe, A. A., Harden, J. W. and Romanovsky, V. E.: Molecular investigations into a globally important carbon pool: Permafrost-protected carbon in Alaskan soils, Global Change Biology, 16(9), 2543-2554, doi: 10.1111/j.1365-2486.2009.02141.x, 2010.

Walz, J., Knoblauch, C., Böhme, L. and Pfeiffer, E. M.: Regulation of soil organic matter decomposition in permafrost-affected Siberian tundra soils - Impact of oxygen availability, freezing and thawing, temperature, and labile organic matter, Soil biology and biochemistry, doi: 10.1016/j.soilbio.2017.03.001, 2017.

Washburn, A. L.: Permafrost Features as Evidence of Climatic Change Earth-Science Reviews, 15, 327-402, doi: 10.1016/0012-8252(80)90114-2, 1980.

Weijers, J. W., Schouten, S., Hopmans, E. C., Geenevasen, J. A., David, O. R., Coleman, J. M., Pancost, R. D. and Sinninghe Damste, J. S.: Membrane lipids of mesophilic anaerobic bacteria thriving in peats have typical archaeal traits, Environmental microbiology, 8(4), 648-657, doi: 10.1111/j.1462-2920.2005.00941.x, 2006.

Wetterich, S., Kuzmina, S., Andreev, A. A., Kienast, F., Meyer, H., Schirrmeister, L., Kuznetsova, T. and Sierralta, M.: Palaeoenvironmental dynamics inferred from late Quaternary permafrost deposits on Kurungnakh Island, Lena Delta, Northeast Siberia, Russia: Quaternary Science Reviews, 27(15), 1523-1540, doi: 10.1016/j.quascirev.2008.04.007, 2008.

Wetterich, S., Schirrmeister, L., Andreev, A. A., Pudenz, M., Plessen, B., Meyer, H. and Kunitsky, V. V.: Eemian and Late Glacial/Holocene palaeoenvironmental records from permafrost sequences at the Dmitry Laptev Strait (NE Siberia, Russia), Palaeogeography, Palaeoclimatology, Palaeoecology, 279(1-2), 73-95, doi: 10.1016/j.palaeo.2009.05.002, 2009.

Wetterich, S., Rudaya, N., Tumskoy, V., Andreev, A. A., Opel, T., Schirrmeister, L. and Meyer, H.: Last Glacial Maximum records in permafrost of the East Siberian Arctic, Quaternary Science Reviews, 30(21-22), 3139-3151, doi: 10.1016/j.quascirev.2011.07.020, 2011.

Wetterich, S., Tumskoy, V., Rudaya, N., Andreev, A. A., Opel, T., Meyer, H., Schirrmeister, L. and Hüls, M.: Ice Complex formation in arctic East Siberia during the MIS3 Interstadial, Quaternary Science Reviews, 84, 39-55, doi: 10.1016/j.quascirev.2013.11.009, 2014.

Wetterich, S., Tumskoy, V., Rudaya, N., Kuznetsov, V., Maksimov, F., Opel, T., Meyer, H., Andreev, A. A. and Schirrmeister, L.: Ice Complex permafrost of MIS5 age in the Dmitry Laptev Strait coastal region (East Siberian Arctic), Quaternary Science Reviews, 147, 298-311, doi: 10.1016/j.quascirev.2015.11.016, 2016.

White, D. C., Davis, W. M., Nickels, J. S., King, J. D. and Bobbie, R. J.: Determination of the sedimentary microbial biomass by extractible lipid phosphate Oecologia, 40(1), 51-62, doi: 10.1007/BF00388810, 1979.

White, R. E.: Principles and practice of soil science: the soil as a natural resource, John Wiley & Sons, 2013.

Xue, K., Yuan, M. M., Shi, Z. J., Qin, Y., Deng, Y., Cheng, L., Liyou, W., He, Z., Van Nostrand, J. D., Bracho, R., Natali, S., Schuur, E. A., Luo, C., Konstantinidis, K. T., Wang, Q., Cole, C. R., Tiedje, J., Luo, Y. and Zhou, J.: Tundra soil carbon is vulnerable to rapid microbial decomposition under climate warming, Nature Climate Change, 6(6), 595-600, doi: 10.1038/nclimate2940, 2016.

Zelles, L.: Fatty acid patterns of phospholipids and lipopolysaccharides in the characterisation of microbial communities in soil: a review, Biol Fertil Soils, 29, 111-129, doi: 10.1007/s003740050533, 1999.

Zimov, S. A., Davydov, S. P., Zimova, G. M., Davydova, A. I., Schuur, E. A. G., Dutta, K. and Chapin III, F. S.: Permafrost carbon: Stock and decomposability of a globally significant carbon pool, Geophysical Research Letters, 33(20), L20502, doi: 10.1029/2006GL027484, 2006.

Zimov, N., Zimov, S., Zimova, A., Zimova, G., Chuprynin, V. and Chapin III, F. S.: Carbon storage in permafrost and soils of the mammoth tundra-steppe biome: Role in the global carbon budget, Geophysical Research Letters, 36(2), doi: 10.1029/2008GL036332, 2009.

Zink, K. G. and Mangelsdorf, K.: Efficient and rapid method for extraction of intact phospholipids from sediments combined with molecular structure elucidation using LC-ESI-MS-MS analysis, Analytical and bioanalytical chemistry, 380(5-6), 798-812, doi:10.1007/s00216-004-2828-2, 2004.

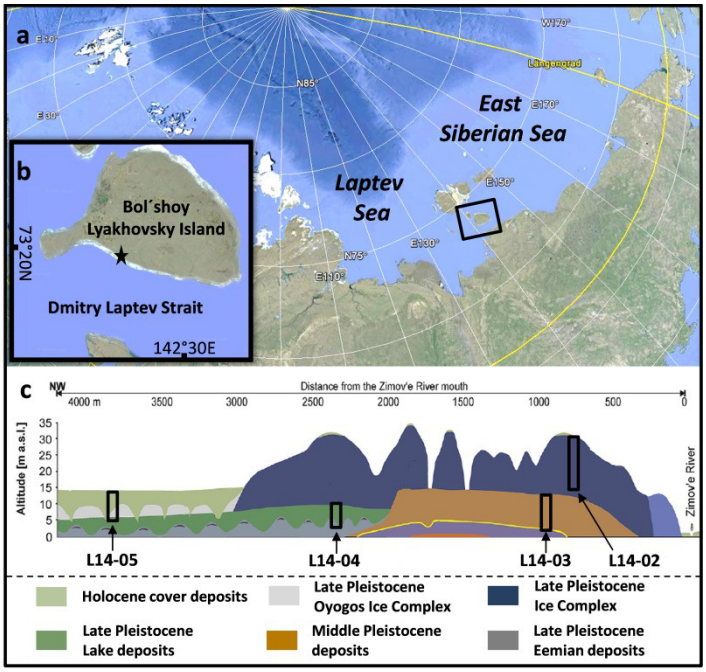

Figure 1: (a) Position of Bol´shoy Lyakhovsky Island in the Siberian Arctic. (b) Study site on Bol´shoy Lyakhovsky Island, indicated by a black star, (c) and location of the drilled cores comprising different age intervals (L14-05, L14-02, L14-03 and L14-04) modified after Wetterich et al. (2014) and Schwamborn and Wetterich (2015).

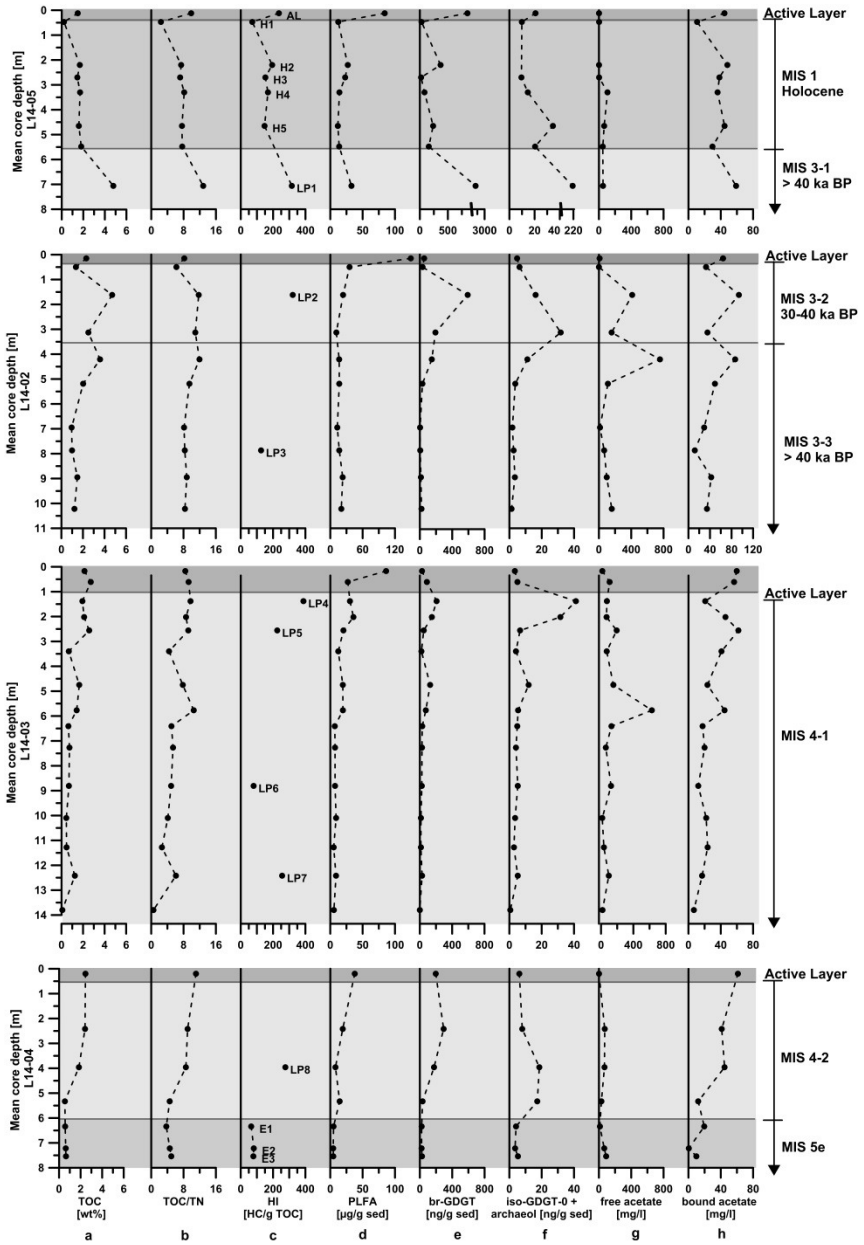

Figure 2: Bio- and geochemical parameters of permafrost cores L14-05, L14-02, L14-03 and L14-04 from Bol´shoy Lyakhovsky Island, northern Siberia, presented with respect to core depth (left axis) and stratigraphic and age units (right column). The vertical profiles show (note partly different axis): a) the total organic carbon (TOC) content in wt%, b) the ratio of total organic carbon and total nitrogen (TOC/TN), c) the hydrogen index (HI) in mg HC/ g TOC, d) concentration of phospholipid fatty acids (PLFAs) in µg/g sediment, e) the concentration of branched glycerol dialkyl glycerol tetraethers (br-GDGTs) in ng/g sediment, f) the concentration of the sum of isoprenoid glycerol dialkyl glycerol tetraether-0 (iso-GDGT-0) in ng/g sediment and archaeol in ng/g sediment, g) the concentration of free acetate in mg/l, and h) concentration of bound acetate in mg/l. Active layer samples are dyed in dark grey, interglacial periods (MIS 1 and MIS 5e) are dyed in grey and the last glacial period (MIS 3 and MIS 4) is dyed in light grey. According to age, stratigraphy and core segments, the MIS 3 unit is subdivided into the core segments MIS 3-1, 3-2 and 3-3, and the MIS 4 unit is subdivided into the core segment MIS 4-1 and 4-2. Sample labels within the HI profile correspond to core samples of different ages (H: Holocene; LP: Late Pleistocene glacial period; E: Eemian).

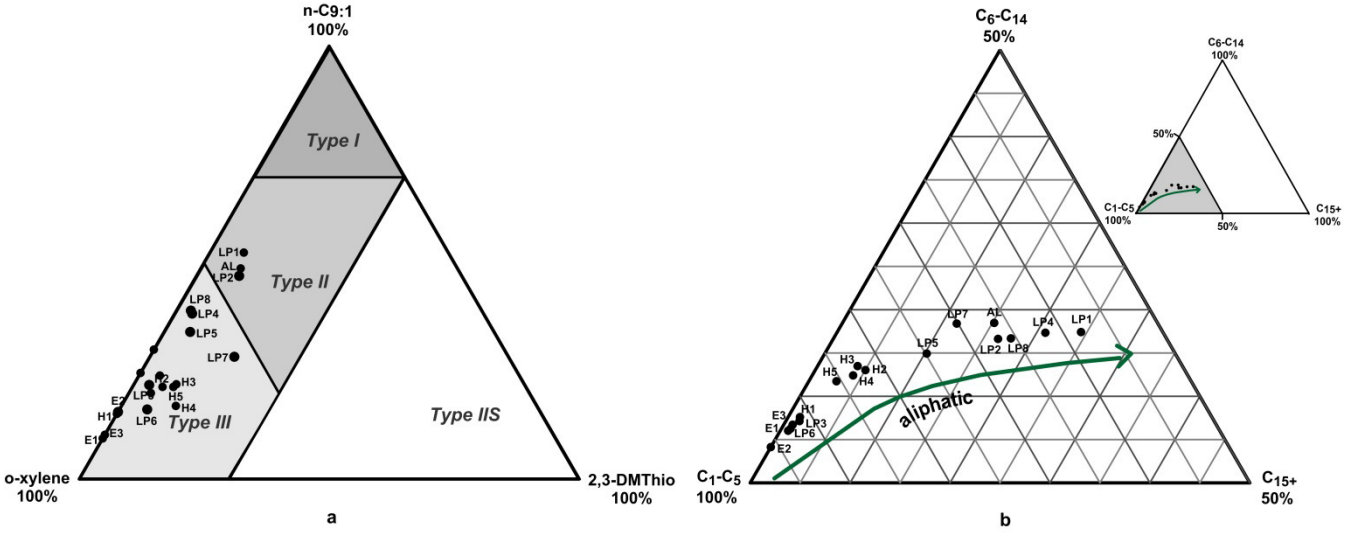

Figure 3: Triangular plots derived from organic matter pyrolysis. (a) Eglinton-diagram: Classification of the kerogen type (type I/II: aquatic and marine; type III: terrestrial; type IIS: enriched sulphur content) due to the relative abundance of 1,2 dimethylbenzene (ortho-xylene), n-nonene (n-C9:1) and 2,3-dimethylthiophene (2,3DMThio) in the OM after Eglinton et al. (1990). (b) Horsfield-diagram: Composition of the OM according to the chain length distribution of short (C1-C5), intermediate (C6-C14) and long (C15+) n-alk-1-enes after Horsfield et al. (1989). The arrow indicates an increasing aliphatic proportion in the OM of the investigated samples. Sample labels correspond to core samples of different ages (H: Holocene; LP: Late Pleistocene glacial period; E: Eemian) with different total organic carbon (TOC) and hydrogen index (HI) values (Fig. 2a,c).

Table 1: Schematic summary of core materials investigated including age periods, marine isotope stage (MIS) after Andreev et al. (2004) and (2009), Wetterich et al. (2004) and (2014), the Russian terms, core numbers and coordinates of drill sites.

Age			Cores	Drilling site
Epoch	MIS	russ.		
Holocene (interglacial)	1	Holocene	L14-05	73.34994° N 141.24156° E
Late Pleistocene Glacial Period (glacial) interstadial	3	Kargin	L14-02	73.33623° N 141.32761° E
Late Pleistocene Glacial Period (glacial) stadial	4	Zyryan	L14-03	73.33464° N 141.32822° E
Eemian (interglacial)	5e	Kazansevo	L14-04	73.34100° N 141.28587° E

Table 2: Schematic summary (from left to right) including age (epoch and marine isotope stage (MIS) classification) after Andreev et al. (2004) and (2009), Wetterich et al. (2004) and (2014), paleo-environment ([1]Schirrmeister et al. (2002), [2]Andreev et al. (2009), [3]Grosse et al. (2007), [4]Sher et al. (2005), [5]Wetterich et al. (2014)), organic matter (OM) quality, substrate potential (present (free acetate) and future (bound acetate)) and core numbers (related to the age classification). To visualize the OM quality and the substrate potential a relative scaling based on the results of this study is used: very good (++), good (+), poor (-) and very poor (--).

Age		Palaeoenvironment	OM quality	Substrate potential		Cores
Epoch	MIS			present	future	
Holocene (interglacial)	1	- climatic warming[1] - moisture increased thawing, thermokarst[2] - unstable environmental conditions[2] - dissected landscape influences by local hydrology[3]	-	- -	+	L14-05
Late Pleistocene Glacial Period (glacial) interstadial	3	- increased temperature and soil moisture[4]	+ +	-	+ +	
		- warm/moderate and dry climate[5] -optimum: warm and dry (48 to 38 ka BP)[5]	+ +	+ +	+ +	L14-02
		- warmer summers, open vegetation[2]	-	+	+	
stadial	4	- cold and dry climate[5] - harsh climate conditions[2] - thin snow cover, low precipitation[2]	+	+	+	L14-03
			-			
			+			L14-04
Eemian (interglacial)	5e	- warmer climate, open-grass tundra similar to modern[2] - permafrost thawing[2] - optimum: 4-5 °C higher summer temperatures than modern, shrub tundra[2]	- -	-	- -	

Table S1: Concentration of identified branched glycerol dialkyl glycerol tetraethers (GDGTs) (GDGT-Ia, GDGT-Ib, GDGT-II, GDGT-III), isoprenoid GDGTs (GDGT-0, GDGT-1, GDGT-2, crenarchaeol), archaeol as well as the calculated branched and isoprenoid tetraether (BIT) index. For GDGT structures please refer to Schouten et al. [2013].

Core name	mean depth [m]	Archaeol [ng/g Sed]	GDGT-0 [ng/g Sed]	GDGT-1 [ng/g Sed]	GDGT-2 [ng/g Sed]	Crenarchaeol [ng/g Sed]	GDGT-Ia [ng/g Sed]	GDGT-Ib [ng/g Sed]	GDGT-II [ng/g Sed]	GDGT-III [ng/g Sed]	BIT
L14-05	0.1	17.7	3.1	0.6	0.6	0.0	125.7	8.2	391.0	309.2	1.0
	0.5	8.9	1.0	0.2	0.1	0.0	2.6	0.5	11.5	15.2	1.0
	2.2	41.1	13.9	2.9	2.2	5.1	39.5	5.9	124.7	180.2	1.0
	2.7	7.5	2.1	0.3	0.2	0.5	2.2	0.5	7.5	10.1	1.0
	3.3	10.0	4.7	0.7	0.5	1.5	9.2	1.4	29.5	38.8	1.0
	4.7	22.0	12.6	2.5	2.7	5.2	21.7	4.0	77.8	121.7	1.0
	5.5	5.4	15.0	3.1	3.5	6.5	20.1	3.6	68.2	68.6	1.0
	7.1	81.1	133.4	5.5	4.6	0.0	269.5	11.0	871.8	918.1	1.0
L14-02	0.2	3.9	0.8	0.0	0.0	0.5	12.9	0.5	24.2	15.4	1.0
	0.5	5.9	0.3	0.0	0.0	0.1	8.2	1.3	16.2	8.5	1.0
	1.6	12.4	3.8	1.1	0.8	1.0	92.1	14.4	278.8	206.0	1.0
	3.1	23.2	8.6	1.7	1.5	2.3	26.2	4.3	70.5	90.8	1.0
	4.2	10.2	0.9	0.5	0.7	1.4	17.1	3.1	68.2	59.3	1.0
	5.2	2.7	0.9	0.3	0.3	0.8	4.2	1.0	14.6	12.2	0.9
	7.0	1.4	0.5	0.2	0.2	0.4	0.8	0.1	1.6	1.2	0.9
	7.9	1.1	1.5	0.4	0.4	1.0	0.9	0.1	2.0	1.7	0.9
	9.0	1.5	1.9	0.5	0.5	0.3	2.6	0.3	5.3	5.4	0.9
	10.2	1.0	0.3	0.0	0.0	0.3	4.6	0.2	9.3	6.8	1.0
L14-03	0.2	2.0	1.4	0.6	0.6	1.8	4.0	0.4	12.1	10.6	0.9
	0.6	4.6	0.4	0.0	0.0	0.1	18.5	0.7	42.1	26.0	1.0
	1.4	38.3	2.8	0.6	0.5	0.0	19.9	1.4	83.7	103.1	1.0
	2.0	28.8	2.8	0.6	0.6	0.2	21.6	1.2	60.5	65.7	1.0
	2.6	5.6	1.0	0.3	0.4	0.6	11.0	0.6	24.6	12.1	1.0
	3.4	3.0	1.1	0.3	0.0	0.4	3.9	0.3	8.7	7.5	1.0
	4.8	10.1	1.8	0.5	0.3	0.4	21.0	2.0	55.4	49.6	1.0
	5.8	4.2	1.3	0.4	0.0	0.6	10.3	1.3	29.4	33.1	1.0
	6.4	3.5	1.4	0.3	0.3	0.5	6.7	0.6	13.3	9.6	1.0
	7.3	2.8	1.3	0.3	0.3	0.6	5.9	0.5	11.8	8.9	1.0
	8.8	3.3	1.9	0.5	0.5	1.1	5.4	0.5	10.9	8.5	1.0
	10.1	2.6	1.0	0.2	0.2	0.4	2.8	0.3	6.2	5.1	1.0
	11.3	2.0	0.8	0.2	0.2	0.3	3.0	0.2	5.9	4.6	1.0
	12.4	3.7	1.5	0.0	0.0	0.5	7.4	0.0	12.6	8.1	1.0
	13.8	0.6	0.0	0.0	0.0	0.0	0.0	0.0	0.0	0.0	1.0
L14-04	0.2	5.2	1.0	0.4	0.3	0.6	34.5	1.0	82.5	78.9	1.0
	2.4	7.0	1.0	0.4	0.3	0.1	55.6	3.9	133.7	100.8	1.0
	4.0	17.4	1.2	0.4	0.4	0.2	29.0	2.2	76.5	67.3	1.0
	5.3	15.8	1.5	0.2	0.2	0.4	2.8	0.5	9.8	21.1	1.0
	6.3	2.9	1.2	0.3	0.3	0.6	3.8	0.4	8.3	10.0	1.0
	7.2	2.5	1.0	0.2	0.2	0.4	3.9	0.4	8.4	9.1	1.0
	7.5	3.4	1.9	0.5	0.5	1.0	5.6	0.5	10.9	10.2	1.0